

Security Assessment of Electricity Distribution Networks under DER Node Compromises

Devendra Shelar and Saurabh Amin

Abstract

This article focuses on the security assessment of electricity distribution networks (DNs) with vulnerable distributed energy resource (DER) nodes. The adversary model is simultaneous compromise of DER nodes by strategic manipulation of generation set-points. The loss to the defender (DN operator) includes loss of voltage regulation and cost of induced load control under supply-demand mismatch caused by the attack. A 3-stage Defender-Attacker-Defender (DAD) game is formulated: in Stage 1, the defender chooses a security strategy to secure a subset of DER nodes; in Stage 2, the attacker compromises a set of vulnerable DERs and injects false generation set-points; in Stage 3, the defender responds by controlling loads and uncompromised DERs. Solving this trilevel optimization problem is hard due to nonlinear power flows and mixed-integer decision variables. To address this challenge, the problem is approximated by tractable formulations based on linear power flows. The set of critical DER nodes and the set-point manipulations characterizing the optimal attack strategy are characterized. An iterative greedy approach to compute attacker-defender strategies for the original nonlinear problem is proposed. These results provide guidelines for optimal security investment and defender response in pre- and post-attack conditions, respectively.

I. INTRODUCTION

Integration of distributed energy resources (DERs) such as solar photovoltaic (PV) and solar thermal power generation with electricity distribution networks (DNs) is a major aspect of smart grid development [1]. Some reports estimate that, by 2050, solar PVs will contribute up to 23.7 % of the total electricity generation in the US. Large-scale deployment of DERs can be utilized to improve grid reliability, reduce dependence on bulk generators (especially, during peak demand), and decrease network losses (at least, up to a certain penetration level) [2]. Harnessing these capabilities requires secure and reliable operation of cyber-physical components such as smart inverters, DER controllers, and communication network between DERs and remote control centers. Thus, reducing security risks is a crucial aspect of the design and operation of DNs [3]–[7]. This article focuses on the problem of security assessment of DNs under threats of DER node disruptions by a malicious adversary.

We are specifically interested in limiting the loss of voltage regulation and supply-demand mismatch that can result from the simultaneous compromise of multiple DERs nodes on a distribution feeder. It is well known that the active power curtailment and reactive power control are two desirable capabilities that can help maintain the operational requirements in DNs with large-scale penetration of DERs with intermittent nature [2], [8], [9]. We investigate the specific ways in which these capabilities need to be built into the DER deployment designs, and show that properly chosen security strategies can protect DNs against a class of security attacks.

Our work is motivated by recent progress in three topics: **(T1)** Interdiction and cascading failure analysis of power grids (especially, transmission networks) [10]–[12]; **(T2)** Cyber-physical security of networked control systems [3]–[6], [13]; and **(T3)** Optimal power flow (OPF) and control of distribution networks with DERs [2], [9], [14].

Existing work in **(T1)** employs state-of-the-art computational methods for solving large-scale, mixed integer programs for interdiction/cascade analysis of transmission networks assuming direct-current (DC) power flow models. Since our focus is on security assessment of DNs, we also need to model reactive power demand, in addition to the active power flows. In this work, we consider standard DN model with constant power loads and DERs [9], [14], but we restrict our attention to tree networks. This enables us to obtain structural results on optimal attack strategies. We show that these structural results also provide guidelines for investment in deploying IT security solutions, especially in geographically diverse DNs.

The adversary model in this paper considers simultaneous DER node compromises by false-data injection attacks. Thanks to the recent progress in **(T2)**, similar models have been proposed for a range of cyber-physical systems [4], [5]. Our model is motivated by the DER failure scenarios proposed by power system security experts [15]. These scenarios consider

Manuscript submitted on May 26, 2015

D. Shelar and S. Amin are with the Department of Civil and Environmental Engineering, Massachusetts Institute of Technology, Cambridge, MA 02139 USA (e-mail: shelard,amins@mit.edu).

This work was supported by EPRI grant for “Modeling the Impact of ICT Failures on the Resilience of Electric Distribution Systems” (contract ID: 10000621), and NSF project “FORCES” (award #: CNS-1239054).

shutdown of DER systems when an external threat agent compromises the DERs by a direct attack, or by manipulating the power generation set-points sent from the control center to individual DER nodes/controllers; see Figure 1. The security threats to DNs are real. The recent cyber attack on Ukraine’s power grid shows that an external attacker can compromise multiple DN components by exploiting commonly known IT vulnerabilities [16]. Another real world attack that is directly related to the attack model introduced in this paper was highlighted in a 2015 Congressional Research Service report [17]. This attack was conducted by computer hackers to obtain a back-door entry to the grid. They exploited the IT systems that enable integration of DERs/renewable energy sources.

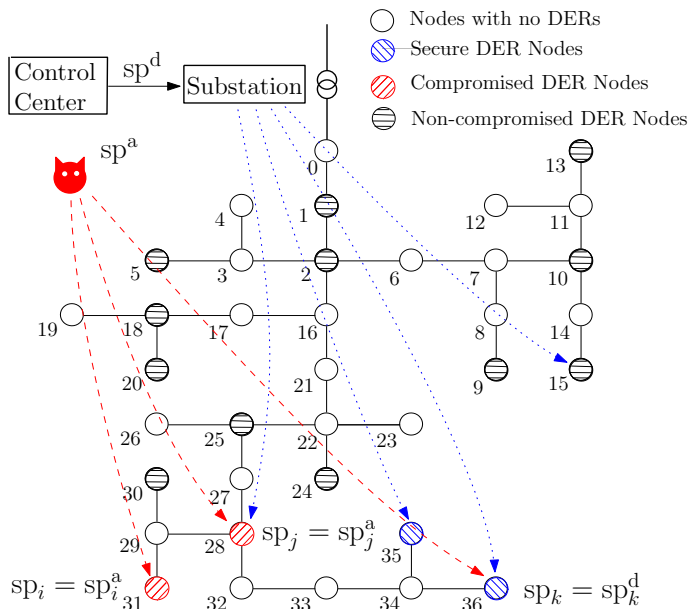


Fig. 1: Illustration of the DER failure scenario proposed in [15] on a modified IEEE 37-node network.

In our model, the attacker’s objective is to impose loss of voltage regulation to the defender (i.e., network operator), and also induce him to exercise load control in order to reduce the supply-demand mismatch immediately after the attack. The defender’s primary concern in post-attack conditions is to reduce the costs due to loss of voltage regulation and load control. Hence, in our model, the line losses are assigned relatively lesser weight. For a fixed attack, solving the problem of defender response via load control and the control of uncompromised DERs is similar to the recent results in **(T3)**, i.e., convex relaxations of OPF problem.

Our main contribution is analysis of a three-stage sequential security game posed in Section II. In Stage 1, the defender invests in securing a subset of DER nodes but cannot ensure security of all nodes due to budget constraints; in Stage 2, the resource-constrained attacker compromises a subset of vulnerable DER nodes and manipulates their set-points; in Stage 3, the defender responds by regulating the supply-demand mismatch. This defender-attacker-defender (DAD) game models both strategic investment decisions (Stage 1) and operation of DN during attacker-defender interaction (Stages 2-3). Solving the DAD game is a hard problem due to nonlinear power flow, DER constraints, and mixed-integer decision variables.

In Section III, we provide tractable approximations of the sub-game induced for a fixed defender security strategy, i.e., the attacker-defender interaction in Stages 2-3; see Theorem 1. These approximations can be efficiently solved, and hold under the assumption of no reverse power flows, small impedances, and small line losses. Next we show structural results for the master-problem (i.e., optimal attack for fixed defender response), and the sub-problem (i.e., optimal defender response for fixed attack). For the master-problem, we derive the false set-points that the attacker will introduce in any compromised DER (Theorem 2), and also propose computational methods to solve for attack vectors, i.e., DER nodes whose compromise will cause maximum loss to the defender (Propositions 3 and 4). For the sub-problem, we utilize the convex relaxations of OPF to compute optimal defender response for a fixed attack (Lemma 3), and under a restricted set of conditions, provide a range of new set-points for the uncompromised DERs (Proposition 2). These results lead to a greedy approach, which efficiently computes the optimal attack and defender response (Algorithm 3). We prove optimality of the greedy approach for DNs with identical resistance-to-reactance ratio (Theorem 3), and show that the approach efficiently obtains optimal attack strategy and defender response for a broad range of conditions (Section V). Thanks to the structural results on optimal attack strategy, our greedy approach has significantly better computational performance than standard techniques to solve bilevel

optimization problems (e.g., Benders decomposition [11]). Finally, we provide a characterization of the optimal security strategy for Stage 1 decision by the defender, albeit for symmetric DNs (Section IV, Theorem 4).

II. PROBLEM FORMULATION

A. Distribution network model

We summarize the standard network model of radial electric distribution systems [18], [19], [20], [9]. Consider a tree network of nodes and distribution lines $\mathcal{G} = (\mathcal{N} \cup \{0\}, \mathcal{E})$, where \mathcal{N} denotes the set of all nodes except the substation (labeled as node 0), and let $N := |\mathcal{N}|$. Let $V_i \in \mathbb{C}$ denote the complex voltage at node i , and $\nu_i := |V_i|^2$ denote the square of voltage magnitude. We assume that the magnitude of substation voltage $|V_0|$ is constant. Let $I_j \in \mathbb{C}$ denote the current flowing from node i to node j on line $(i, j) \in \mathcal{E}$, and $\ell_j := |I_j|^2$ the square of the magnitude of the current. A distribution line $(i, j) \in \mathcal{E}$ has a complex impedance $z_j = r_j + \mathbf{j}x_j$, where $r_j > 0$ and $x_j > 0$ denote the resistance and inductance of the line (i, j) , respectively, and $\mathbf{j} = \sqrt{-1}$.

The voltage regulation requirements of the DN under *nominal* no attack conditions govern that:

$$\forall i \in \mathcal{N}, \quad \underline{\nu}_i \leq \nu_i \leq \bar{\nu}_i, \quad (1)$$

where $\underline{\nu}_i = |\underline{V}_i|^2$ and $\bar{\nu}_i = |\bar{V}_i|^2$ are the *soft* lower and upper bounds for maintaining voltage quality at node i . Additionally, voltage magnitudes under *all* conditions satisfy:

$$\forall i \in \mathcal{N}, \quad \underline{\mu} \leq \nu_i \leq \bar{\mu}, \quad (2)$$

where $\underline{\mu}$ and $\bar{\mu}$ are the *hard* voltage safety bounds for any nodal voltage, and $0 < \underline{\mu} < \min_{i \in \mathcal{N}} \underline{\nu}_i \leq \max_{i \in \mathcal{N}} \bar{\nu}_i < \bar{\mu}$.

1) Load model: We consider constant power loads [21].¹ Let $sc_i := pc_i + \mathbf{j}qc_i$ denote the power consumed by a load at node i , where pc_i and qc_i are the real and reactive components. Let $sc_i^{\text{nom}} := pc_i^{\text{nom}} + \mathbf{j}qc_i^{\text{nom}}$ denote the *nominal* power demanded by a node i , where pc_i^{nom} and qc_i^{nom} are the real and reactive components of sc_i^{nom} . Under our assumptions, for all $i \in \mathcal{N}$, $pc_i \leq pc_i^{\text{nom}}$ and $qc_i \leq qc_i^{\text{nom}}$, i.e., the actual power consumed at each node is upper bounded by the nominal demand:

$$\forall i \in \mathcal{N}, \quad sc_i \leq sc_i^{\text{nom}}. \quad (3)$$

2) DER model:² Let $sg_i := pg_i + \mathbf{j}qg_i$ denote the power generated by the DER connected to node i , where pg_i and qg_i denote the active and reactive power, respectively. Following [14], [9], sg_i is bounded by the apparent power capability of the inverter, which is a given constant \bar{sp}_i . We denote the DER set-point by $sp_i = \mathbf{Re}(sp_i) + \mathbf{j}\mathbf{Im}(sp_i)$, where $\mathbf{Re}(sp_i)$ and $\mathbf{Im}(sp_i)$ are the real and reactive components. The power generated at each node is constrained as follows:

$$\forall i \in \mathcal{N}, \quad sg_i \leq sp_i \in \mathcal{S}_i, \quad (4)$$

where $\mathcal{S}_i := \{sp_i \in \mathbb{C} \mid \mathbf{Re}(sp_i) \geq 0 \text{ and } |sp_i| \leq \bar{sp}_i\}$. $\mathcal{S} := \prod_{i \in \mathcal{N}} \mathcal{S}_i$ denotes the set of configurable set-points.

We denote the net power consumed at node i by $s_i := sc_i - sg_i$. A DN can be fully specified by the tuple $\langle \mathcal{G}, |V_0|, z, sc^{\text{nom}}, \bar{sp} \rangle$, where $z, sc^{\text{nom}}, \bar{sp}$ are row vectors of appropriate dimensions, and are assumed to be constant.

3) Power flow equations: The 3-phase balanced nonlinear power flow (NPF) on line $(i, j) \in \mathcal{E}$ is given by [18]:

$$S_j = \sum_{k:(j,k) \in \mathcal{E}} S_k + sc_j - sg_j + z_j \ell_j \quad (5a)$$

$$\nu_j = \nu_i - 2\mathbf{Re}(\bar{z}_j S_j) + |z_j|^2 \ell_j \quad (5b)$$

$$\ell_j = \frac{|S_j|^2}{\nu_i}, \quad (5c)$$

where $S_j = P_j + \mathbf{j}Q_j$ denotes the complex power flowing from node i to node j on line $(i, j) \in \mathcal{E}$, and \bar{z} is the complex conjugate of z ; (5a) is the power conservation equation; (5b) relates the voltage drop and the power flows; and (5c) is the current-voltage-power relationship. For the NPF model (5), we define a state as follows:

$$\mathbf{x} := [\nu, \ell, sc, sg, S],$$

¹We do not consider frequency dependent loads as our analysis is limited to attacks that do not cause disturbances in system frequency; see § II-D for our justification of constant system frequency assumption.

²We use the term DER to denote the complete DER-inverter assembly attached to a node of DN.

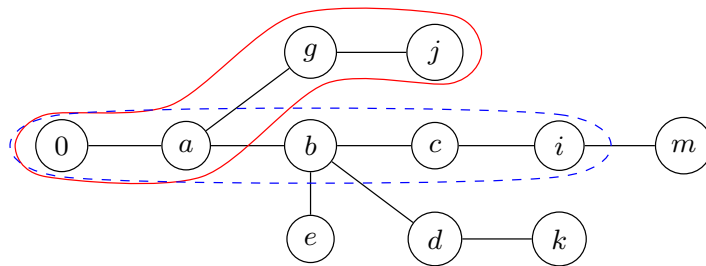


Fig. 2: Precedence description of the nodes for a tree network. Here, $j <_i k$, $e =_i k$, $b < k$, $\mathcal{P}_j = \{a, g, j\}$, $\mathcal{P}_i \cap \mathcal{P}_j = \{a\}$.

where $x \in \mathbb{R}_+^{2N} \times \mathbb{C}^{3N}$, and ν , ℓ , sc , sg , and S are row vectors of appropriate dimensions. Let \mathcal{F} denote the set of all states x that satisfy (2), (3), (4) and the NPF model (5), and define the set of all states with *no reverse power flows* as follows:

$$\mathcal{X} := \{x \in \mathcal{F} | S \geq 0\}.$$

The linear power flow (LPF) approximation of (5) is:

$$\hat{S}_j = \sum_{k:(j,k) \in \mathcal{E}} \hat{S}_k + \hat{sc}_j - \hat{sg}_j \quad (6a)$$

$$\hat{\nu}_j = \hat{\nu}_i - 2\mathbf{Re}(\bar{z}_j \hat{S}_j) \quad (6b)$$

$$\hat{\ell}_j = \frac{|\hat{S}_j|^2}{\hat{\nu}_i}, \quad (6c)$$

where $\hat{x} := [\hat{\nu}, \hat{\ell}, \hat{sc}, \hat{sg}, \hat{S}]$ is a state of the LPF model, and analogous to the NPF model, define the set of LPF states $\hat{\mathcal{X}}$ with no reverse power flows as $\hat{\mathcal{X}}$.

B. Notation and definitions

All vectors are row vectors, unless otherwise stated. For two vectors c and d , $c \odot d$ denotes their Hadamard product.

Let $K_j := \frac{r_j}{x_j}$ be the resistance-to-reactance (\mathbf{r}/\mathbf{x}) ratio for line $(i, j) \in \mathcal{E}$, and let \underline{K} and \overline{K} denote the minimum and maximum of the K_j s over all $(i, j) \in \mathcal{E}$. We say that DERs at nodes j and k are homogeneous with respect to each other if their set-point configurations as well as their apparent power capabilities are identical, i.e., $sp_j = sp_k$ and $\overline{sp}_j = \overline{sp}_k$. Similarly, two loads at nodes j and k are homogeneous if $sc_j^{\text{nom}} = sc_k^{\text{nom}}$.

For any given node $i \in \mathcal{N}$, let \mathcal{P}_i be the path from the root node to node i . Thus, \mathcal{P}_i is an ordered set of nodes starting from the root node and ending at node i , excluding the root node; see Fig. 2. We say that node j is an *ancestor* of node k ($j < k$), or equivalently, k is a successor of j iff $\mathcal{P}_j \subset \mathcal{P}_k$. We define the *relative ordering* \leq_i , with respect to a ‘‘pivot’’ node i as follows:

- j precedes k ($j \leq_i k$) iff $\mathcal{P}_i \cap \mathcal{P}_j \subseteq \mathcal{P}_i \cap \mathcal{P}_k$.
- j strictly precedes k ($j <_i k$) iff $\mathcal{P}_i \cap \mathcal{P}_j \subset \mathcal{P}_i \cap \mathcal{P}_k$.
- j is at the same precedence level as k ($j =_i k$) iff $\mathcal{P}_i \cap \mathcal{P}_j = \mathcal{P}_i \cap \mathcal{P}_k$.

We define the common path impedance between any two nodes $i, j \in \mathcal{N}$ as the sum of impedances of the lines in the intersection of paths \mathcal{P}_i and \mathcal{P}_j , i.e., $Z_{ij} := \sum_{k \in \mathcal{P}_i \cap \mathcal{P}_j} z_k$, and denote the resistive (real) and inductive (imaginary) components of Z_{ij} by R_{ij} and X_{ij} , respectively.

Finally, we define some useful terminology for the tree network \mathcal{G} . Let H denote the height of \mathcal{G} , and let \mathcal{N}_h denote the set of nodes on level h for $h = 1, 2, \dots, H$. For any node $i \in \mathcal{N}$, h_i denotes the level of node i ; \mathcal{N}_i^c the set of children nodes of node i ; Λ_i the set of nodes in the subtree rooted at node i ; Λ_i^j the set of nodes in the subtree rooted at node i until level h_j , where $j \in \Lambda_i$; \mathcal{N}_L the set of leaf nodes, i.e., $\mathcal{N}_L := \{j \in \mathcal{N} \mid \nexists k \in \mathcal{N} \text{ s.t. } (j, k) \in \mathcal{E}\}$.

C. Defender-Attacker-Defender security game

We consider a 3-stage sequential game between a defender (network operator) and an attacker (external threat agent).

- **Stage 1:** The defender chooses a security strategy $u \in \mathcal{U}_B$ to secure a subset of DERs;
- **Stage 2:** The attacker chooses from the set of DERs that were not secured by the defender in Stage 1, and manipulates their set-points according to a strategy

$$\psi := [\text{sp}^a, \delta] \in \Psi_M(u);$$

- **Stage 3:** The defender responds by choosing the set-points of the uncompromised DERs and, if possible, impose load control at one or more nodes according to a strategy $\phi := [\text{sp}^d, \gamma] \in \Phi(u, \psi)$.

The [DAD] game is a sequential game of perfect information, i.e. each player is perfectly informed about the actions that have been chosen by the previous players. The equilibrium concept is the classical Stackelberg equilibrium.

In this game, \mathcal{U}_B and $\Phi(u, \psi)$ denote the set of defender actions in Stage 1 and 3, respectively; and $\Psi_M(u)$ denotes the set of attacker strategies in Stage 2. Formally, the defender-attacker-defender [DAD] game is as follows:

$$\text{[DAD]} \mathcal{L} := \min_{u \in \mathcal{U}_B} \max_{\psi \in \Psi_M} \min_{\phi \in \Phi} L(x(u, \psi, \phi)) \quad (7)$$

$$\text{s.t. } x(u, \psi, \phi) \in \mathcal{X} \quad (8a)$$

$$sc(u, \psi, \phi) = \gamma \odot sc^{\text{nom}} \quad (8b)$$

$$sg(u, \psi, \phi) = u \odot \text{sp}^d + (\mathbf{1}_N - u) \odot [\delta \odot \text{sp}^a + (\mathbf{1}_N - \delta) \odot \text{sp}^d], \quad (8c)$$

where (8b) specifies that the *actual power consumed* at node i is equal to the power demand scaled by the corresponding load control parameter $\gamma_i \in [\underline{\gamma}_i, 1]$ chosen by the defender.

The constraint (8c) models the net effect of defender choice u_i in Stage 1, the attacker choice $(\text{sp}_i^a, \delta_i)$ in Stage 2, and the defender choice sp_i^d in Stage 3 on the *actual power generated* at node i . Thus, (8c) is the *adversary model* of [DAD] game: the DER i is compromised *if and only if* it was not secured by the defender ($u_i = 0$) *and* was targeted by the attacker ($\delta_i = 1$). Specifically, if i is compromised, $\text{sp}_i = \text{sp}_i^a$, where $\text{sp}_i^a = \mathbf{Re}(\text{sp}_i^a) + \mathbf{jIm}(\text{sp}_i^a)$ is the false set-point chosen by the attacker. The set-points of non-compromised DERs are governed by the defender, i.e., if DER i is not compromised $\text{sp}_i = \text{sp}_i^d$.

Note that the physical restriction (4) applies to all DER nodes, including the compromised ones. If the attacker's set-point violates this constraint, it will not be admitted by the inverter as a valid set-point. Such an attack will not affect the attack model (8c), and consequently it will not change the actual power generated by the DER. Also, our adversary model assumes that the DER's power output, sg , quickly attain the set-points specified by (8c), i.e., the model does not consider dynamic set-point tracking.³

During the nominal operating conditions, the network operator minimizes the line losses due to power flow on the distribution lines (L_{LL}). Typical OPF formulations mainly account for this cost. However, this objective function is not representative of the loss incurred by operator (defender) during a cyber-physical attack on the DN. We define loss function in [DAD] as follows:

$$L(x(u, \psi, \phi)) := L_{VR}(x) + L_{LC}(x) + L_{LL}(x), \quad (9)$$

where $L_{VR}(x)$ and $L_{LC}(x)$ model the *monetary cost* to the defender due to the loss in voltage regulation and the cost of load curtailment/shedding (i.e., loss due to partially satisfied demand), respectively. The term denotes L_{LL} the total line losses. These costs are defined as follows:

$$L_{VR}(x) := \|W \odot (\underline{\nu} - \nu)_+\|_\infty \quad (10a)$$

$$L_{LC}(x) := \|C \odot (1 - \gamma) \odot pc^{\text{nom}}\|_1 \quad (10b)$$

$$L_{LL}(x) := \|r \odot \ell\|_1, \quad (10c)$$

where $W, C \in \mathbb{R}_+^N$. The weight W_i is the cost of unit voltage bound violation and C_i is the cost of shedding unit load (or demand dissatisfaction) at node i , and r denotes the vector of resistances. Note that L_{VR} is the maximum of the weighted non-negative difference between the lower bound $\underline{\nu}_i$ and nodal voltage square ν_i . We expect that during the attack, the defender's primary concern will be to satisfy the voltage regulation requirements, and minimize the inconvenience to the customers due to load curtailment. Thus, we assume that the weights W_i and C_i are chosen such that L_{LL} is relatively small compared to L_{VR} and L_{LC} .

We added the $L_{LL}(x)$ term in (9) primarily to ensure that the loss function $L(x)$ remains strictly convex function of the net demand $s = sc - sg$. The strict convexity allows us to have a unique solution for the inner problem for fixed attacker's

³Note that, under this adversary model, the impact of DER compromise is different than the impact of a natural event, e.g. cloud cover, during which $pg = \mathbf{0}$. The reactive power contribution may be non-negative during a natural event; however, as we show in § III-C, a compromised DER always contributes reactive power equal to the negative of apparent power capability to the DN.

actions. In our computational study in Section V, we choose the weights W and C such that the line loss is negligible compared to L_{VR} and L_{LC} .

More generally, the loss function $L(x)$ should reflect the monetary costs incurred by the defender in maintaining the supply-demand balance and in restoring the safe operating conditions after the attack. Such a general model will contain following terms: (a) the cost of supplying additional power from the substation node to match the difference between actual power consumed by the loads and the effective DER generation ($L_S(x)$); (b) the cost due to the loss of voltage regulation ($L_{VR}(x)$); (c) the cost of curtailing or shedding certain loads ($L_{LC}(x)$); (d) the cost of reactive power (VAR) control and the cost of energy spillage for the uncompromised DERs ($L_{AC}(x)$); and (e) the costs of equipment damage due to the attack ($L_D(x)$).

For the sake of simplicity, we do not consider $L_{AC}(x)$ and $L_D(x)$ in our formulation. The choice of ignoring $L_{AC}(x)$ can be justified if we assume that the DER owners participate in VAR control, perhaps in return of a pre-specified compensation by the operator/defender. Alternatively, the DERs may be required to contribute reactive power during contingency scenarios (i.e., supply-demand mismatch during the attack). The main difficulty in modeling $L_D(x)$ is that it requires relating the state vector to the probability of equipment failures. Since our focus is on security assessment of DNs, as opposed to network reinforcement using investment in physical protection devices, we ignore this cost in our analysis. Finally, we also ignore the contribution of $L_S(x)$ to the loss function, as it is likely to be dominated by L_{VR} and L_{LC} .

Stage 1 [Security Investment]: The set of defender actions is:

$$\mathcal{U}_B := \{u \in \{0, 1\}^{\mathcal{N}} \mid \|u\|_0 \leq B\},$$

where $B \leq |\mathcal{N}|$ denotes a security budget. Since, securing control-center's communication to every DER node in a geographically diverse DN might be costly/impractical, we impose that the maximum number of nodes the defender can secure is B . A defender's choice $u \in \mathcal{U}_B$ implies that a DER at node i is secure if $u_i = 1$ (i.e. DER at node i cannot be compromised), and vulnerable to attack if $u_i = 0$. Let $\mathcal{N}_s(u) := \{i \in \mathcal{N} \mid u_i = 1\}$ and $\mathcal{N}_v(u) := \mathcal{N} \setminus \mathcal{N}_s(u)$ denote the set of secure and vulnerable nodes, for a given u .⁴

There are several factors which limit the defender's ability to ensure full security of DERs. First, to ensure the security of control software and network communications that support DER operations, we need cost-effective and interoperable security solutions that can be widely adopted by different entities (e.g., DER manufacturers, service providers, and owners). Also securing control center's communication to every DER node in a geographically diverse DN might be costly/impractical. Secondly, the DNs are likely to inherit some of the vulnerabilities of COTS IT devices that may directly or indirectly affect DER operations. Third, the defenders (operators) need to justify the business case to deploy security solutions. Existing work on security investments in such networked environments, indicates that the operators tend to underestimate security risks [22]. Consequently, in the absence of proper regulatory impositions, they tend to underinvest in well-known security solutions. In our model, we capture the limitations imposed by these factors by introducing a security budget B which restricts the maximum number of nodes the defender can secure in Stage 1.

Stage 2 [Attack]: Let $\Psi_M(u) := \mathcal{S}(u) \times \mathcal{D}_M(u)$ denotes the set of attacker actions for a defender's choice u , where

$$\begin{aligned} \mathcal{S}(u) &:= \prod_{i \in \mathcal{N}_v(u)} \mathcal{S}_i \times \prod_{j \in \mathcal{N}_s(u)} \{0 + 0j\} \\ \mathcal{D}_M(u) &:= \{\delta \in \{0, 1\}^{\mathcal{N}} \mid \delta \leq \mathbf{1}_N - u, \|\delta\|_0 \leq M\}, \end{aligned}$$

and $M \leq |\mathcal{N}_v|$ is the maximum number of DERs that the attacker can compromise. This limit accounts for the attacker's resource constraints (and/or restrict his influence based on his knowledge of DER vulnerabilities). The attacker *simultaneously* compromises a subset of vulnerable DER nodes by introducing incorrect set-points (see the adversary model (8c)), and increase the loss L (see (9)). The attacker's choice is denoted by $\psi := [\text{sp}^a, \delta] \in \Psi_M(u)$, where sp^a denotes the vector of incorrect set-points chosen by the attacker, and $\delta \in \mathcal{D}_M$ denotes the attack vector that indicates the subset of DERs compromised. A DER at node i is compromised if $\delta_i = 1$, and not compromised if $\delta_i = 0$.

We assume that the attacker has full information about the DN, i.e., she knows $\langle \mathcal{G}, |V_0|, z, \text{sc}^{\text{nom}}, \text{sp} \rangle$ and maximum fraction of controllable load at each node. The attacker also knows the set of DERs secured by the defender in Stage 1 of the game, voltage regulation bounds, and defender's cost parameters (i.e. the weight W_i for voltage bound violation and the cost of unit load shedding C_i for each node i). By assuming an informed attacker, we are able to focus on how the attacker

⁴Note that when we say a node is secure, we mean that the DER at that node is not prone to compromise by the attacker. From a practical viewpoint, the defender can secure a DER node by investing in node security solutions such as installing intrusion prevention/detection systems (IPS/IDS) [13]. These security solutions are complementary to the device hardening technologies that can secure the DER-inverter assembly. Our focus is on security against an external threat agent interested in simultaneously compromising multiple DERs. Thus, we restrict our attention to node security solutions.

uses the knowledge of the physical system toward achieving her objective. Thus, we take a conservative approach on security assessment and do not explicitly consider particular mechanisms of how a security vulnerability might be exploited by the attacker. Admittedly, our attack model may be unrealistic in some scenarios; however, it allows us to identify the critical DER nodes, and characterize optimal security investment and defender response; see Sec. IV.

Next, we justify the attacker's resource constraint M . First, the DERs are likely to be heterogeneous in their capacity, design, and manufacturer type. The attacker may not have the specific knowledge to exploit vulnerabilities in all DER systems deployed on a DN. Secondly, in practice, the process of DER integration is gradual and so is the progress on implementing security solutions in the cyber-physical components that support DER operations. The attacker's capability to compromise DERs depends on how the available threat channels vary which such a technological change. Third, the security of DNs is likely to be affected by the security practices adopted by owners of DERs. For example, the attacker's capability will be limited if the DER operations are secured by a regulated distribution utility who faces compliance checks or mandatory disclosure of known incidents. In contrast, he is more likely to gain a backdoor entry if the DN has substantial participation from a variety of third party DER owners who may not follow prudent security practices. In our analysis, we model the attacker's capability by introducing a parameter M which is the maximum number of DERs that the attacker can compromise.

Stage 3 [Defender Response]: Let $\underline{\gamma}_i \geq 0$ denote the maximum permissible fraction of load control at node i , and define the set of Stage 3 defender actions:

$$\Phi(u, \psi) := \mathcal{S} \times \Gamma,$$

where $\Gamma := \prod_{i \in \mathcal{N}} [\underline{\gamma}_i, 1]$. The defender chooses new set-points sp^d of non-compromised DERs, and load control parameters γ_i to reduce the loss L . The defender action is modeled as a vector $\phi := [\text{sp}^d, \gamma] \in \Phi(u, \psi)$, where sp^d (resp. γ) denotes the vector of sp_i^d (resp. γ_i).

We make the standard assumption that the defender knows the nominal demand (i.e., the demand in pre-attack conditions) using measurements collected from the DN nodes. We also assume that the defender can distinguish between compromised and non-compromised DERs. In heavy loading conditions, the defender expects the output of a non-compromised DER to lie in the first quadrant, i.e. it contributes positive active and reactive power to the DN. A simple technique to detect compromised DERs is whether the inverter output lies in the fourth quadrant (see Theorem 2).

D. Assumptions

In general, [DAD] is a non-convex, non-linear, tri-level optimization problem with mixed-integer decision variables. Hence, it is a computationally hard problem. Our goals are:

- (i) to provide structural insights about the optimal attacker and defender strategies of the [DAD] game;
- (ii) to approximate the non-linear (hard) problem by formulating computationally tractable variants based on linear power flow models.

To address these goals we make the following assumptions:

(A0)₀ Voltage quality: In no attack (nominal) conditions, both \mathcal{X} and $\hat{\mathcal{X}}$ satisfy the voltage quality bounds (1).

(A0)₁ Safety: Safety bounds (2) are always satisfied, i.e., $\forall (u, \psi, \phi) \in \mathcal{U}_B \times \Psi \times \Phi, \forall \mathbf{x}(u, \psi, \phi) \in \mathcal{X}, \underline{\mu} \mathbf{1}_N \leq \nu \leq \bar{\mu} \mathbf{1}_N$.

(A0)₂ No reverse power flows: Power flows from node 0 towards the downstream nodes, i.e., $\hat{S} \geq 0$. This implies that $\forall \hat{\mathbf{x}} \in \hat{\mathcal{X}}, \hat{\mathbf{v}} \leq \nu_0 \mathbf{1}_N$; similarly, for NPF model.

(A0)₃ Small impedance: All power flows are in the per unit (*p.u.*) system, i.e., $\nu_0 = 1$ and $\forall (i, j) \in \mathcal{E}, |S_j| < 1$. Furthermore, the resistances and reactances are small, i.e.,

$$\forall (i, j) \in \mathcal{E}, r_j \leq \frac{\underline{\mu}^2}{4\underline{\mu} + 8} < 1, x_j \leq \frac{\underline{\mu}^2}{4\underline{\mu} + 8} < 1,$$

and the common path resistances and reactances are also smaller than 1, i.e., $R_{ii} \leq 1$ and $X_{ii} \leq 1 \forall i \in \mathcal{N}$.

(A0)₄ Small line losses: The line losses are very small compared to the power flows, i.e., $\forall \mathbf{x} \in \mathcal{X}, z \odot \ell \leq \epsilon_0 S$, where ϵ_0 is a small positive number.⁵

(A0)₀-(A0)₁ are standard assumptions. **(A0)₂** assumes that the DER penetration level is such that the net demand is always positive. In real-world DNs, both r_j s and x_j s are typically around 0.01 **(A0)₃**. Also, residential load power factors

⁵Equivalently, ϵ_0 is an upper bound on the maximum ratio of the magnitudes of line losses and the power flows, i.e., $\epsilon_0 = \max_{(i,j) \in \mathcal{E}, P_j \neq 0, Q_j \neq 0} \max \left(\frac{r_j \ell_j}{P_j}, \frac{x_j \ell_j}{Q_j} \right)$. Thus, ϵ_0 can be determined by setting the values of nodal loads to the corresponding nominal demands, and then computing the line losses and power flows for the nominal condition.

$(\frac{pc_j}{|sc_j|})$ are in range of 0.88-0.95. For these values, one can show that $\epsilon_0 \approx 0.05$ **(A0)**₄. We will denote **(A0)**₀-**(A0)**₄ by **(A0)**.

In addition to the aforementioned assumption, we also assume that (a) the node 0 is an infinite bus; (b) the voltage ν_0 is constant, and (c) the system frequency is constant.

We justify these assumptions as follows: Our focus is on the security assessment of DNs that have substation nodes with high enough ramp rates in supplying ~ 50 MW power (typical for medium-voltage (MV) substations). That is, any supply-demand imbalance of the order of 50 MW can be cleared relatively quickly by the substation; hence the infinite substation bus assumption.

The assumption (b) is typical in OPF formulations and we make it for the sake of mathematical convenience. Indeed, as a consequence of attack, there will be a net reduction in the substation voltage relative to the pre-attack value ν_0 . This effect is due to a higher net demand after the Stage 3 of the game. To meet this additional demand, higher currents will flow through the distribution lines, resulting in even higher drops in the nodal voltages than what we obtained using the computational approach detailed in Sec. III-C. Thus, our estimate of the optimal loss is actually a lower bound on the true value of optimal loss that the defender would face when the substation voltage drops after the attack.

To justify assumption (c), we argue that even large-scale penetration of DERs is not likely to achieve a generation capacity beyond 50 MW from a single DN. Even in the worst case, i.e. when all the DERs are simultaneously disconnected, their impact on the system frequency will be negligible.

For the loss of frequency regulation to become a substantive issue for the defender, the DER disruptions need to be systemic. Examples of such attacks include simultaneous compromise of a large number of DERs in multiple DNs attached to a transmission grid, and DER disruptions in a microgrid where immediate connection to a bulk supply source is not possible. In our follow-up work (initiated after the completion of the current manuscript), we began to explore the effects of such attacks on the system frequency by relaxing the infinite bus assumption [23].

Now, we choose ϵ as follows

$$\epsilon := (1 - \epsilon_0)^{-H} - 1, \quad (11)$$

where H is the height of the tree DN and ϵ_0 is chosen as above. Consider another linear power flow model (which we call the ϵ -LPF model):

$$\check{S}_j = \sum_{k:(j,k) \in \mathcal{E}} \check{S}_k + (1 + \epsilon)(\check{sc}_j - \check{sg}_j) \quad (12a)$$

$$\check{\nu}_j = \check{\nu}_i - 2\text{Re}(\check{z}_j \check{S}_j) \quad (12b)$$

$$\check{\ell}_j = \frac{|\check{S}_j|^2}{\check{\nu}_i}, \quad (12c)$$

and $\check{\mathbf{x}} := [\check{\nu}, \check{\ell}, \check{sc}, \check{sg}, \check{S}]$ is a state of ϵ -LPF model, and $\check{\mathcal{X}}$ is the set of all states $\check{\mathbf{x}}$ with no reverse power flows. For $\epsilon = 0$, (12) becomes (6).

We note that both LPF and ϵ -LPF models ignore the line losses term $z_j \ell_j$ in the power balance equation (5a), and the term $|z_j|^2 \ell_j$ in the voltage drop equation (5b). The power flows obtained by ignoring these terms approximate the non-linear power flow (NPF) model calculations under the assumption **(A0)**₃, i.e., the line impedances are very small $|z_j| \ll 1$. Under the assumption **(A0)**₂, i.e. no reverse power flows, the LPF provides a lower bound on the line power flows, and an upper bound on the nodal voltages of the standard DistFlow model [21], [14]. The main use of ϵ -LPF model is that it provides an upper bound on the line power flows and a lower bound on the nodal voltages; see Proposition 1 in Sec. III-A.

We will consider two variants of the [DAD] game (7)-(8):

$$[\widehat{\text{DAD}}] \widehat{\mathcal{L}} := \min_{u \in \mathcal{U}_B} \max_{\psi \in \Psi_M} \min_{\phi \in \Phi} \widehat{L}(\widehat{\mathbf{x}}(u, \psi, \phi))$$

$$\text{s.t. } \widehat{\mathbf{x}}(u, \psi, \phi) \in \widehat{\mathcal{X}}, \quad (8b), (8c)$$

$$[\widetilde{\text{DAD}}] \widetilde{\mathcal{L}} := \min_{u \in \mathcal{U}_B} \max_{\psi \in \Psi_M} \min_{\phi \in \Phi} \widetilde{L}(\widetilde{\mathbf{x}}(u, \psi, \phi))$$

$$\text{s.t. } \widetilde{\mathbf{x}}(u, \psi, \phi) \in \widetilde{\mathcal{X}}, \quad (8b), (8c)$$

where $\widehat{L}(\widehat{\mathbf{x}}) := L_{\text{VR}}(\widehat{\mathbf{x}}) + L_{\text{LC}}(\widehat{\mathbf{x}})$, and $\widetilde{L}(\widetilde{\mathbf{x}}) := L_{\text{VR}}(\widetilde{\mathbf{x}}) + L_{\text{LC}}(\widetilde{\mathbf{x}})$ are the loss functions for $[\widehat{\text{DAD}}]$ and $[\widetilde{\text{DAD}}]$, respectively. Note that the loss functions \widehat{L} and \widetilde{L} do not have the line losses term. The optimal loss L of $[\widehat{\text{DAD}}]$ and $[\widetilde{\text{DAD}}]$ are

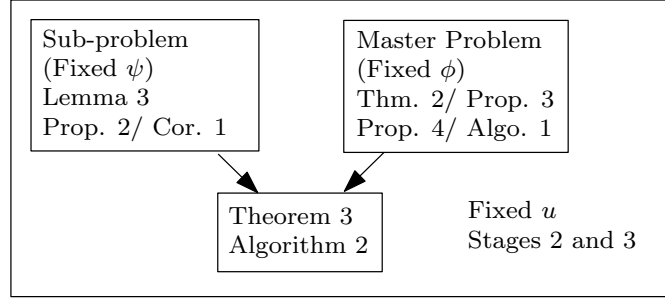


Fig. 3: Outline of Technical Results in Section III

denoted by $\hat{\mathcal{L}}$ and $\check{\mathcal{L}}$, respectively. Our results in §III-IV show that $[\widehat{\text{DAD}}]$ (resp. $[\widetilde{\text{DAD}}]$) help provide under (resp. over) approximation of $[\text{DAD}]$; and the derivation of structural properties of optimal strategies in both $[\widehat{\text{DAD}}]$ and $[\widetilde{\text{DAD}}]$ is analogous to one another.

We will, henceforth, abuse the notation, and use Ψ and Φ to denote $\Psi_{\text{M}}(u)$ and $\Phi(u, \psi)$, respectively. For a summary of notations, see Table III in appendix.

In the following, the reader should note that the proofs of Lemmas 1 to 4 and Propositions 2 to 5 and 7 to 9 are provided in the online supplementary material to this article [24].

III. ATTACKER-DEFENDER SUB-GAME

In this section, we consider the sub-game (Stages 2 and 3) induced by a fixed defender security strategy u in Stage 1:

$$[\text{AD}] \quad \mathcal{L}^u := \max_{\psi \in \Psi} \min_{\phi \in \Phi} L(x(u, \psi, \phi)) \quad \text{s.t.} \quad (8)$$

Analogous to the variants of $[\text{DAD}]$, $[\widehat{\text{DAD}}]$ and $[\widetilde{\text{DAD}}]$, we define two variants of the sub-game $[\text{AD}]$: $[\widehat{\text{AD}}]$ (resp. $[\widetilde{\text{AD}}]$) with $\hat{\mathcal{X}}$ (resp. $\check{\mathcal{X}}$) in (8a). The optimal losses of $[\widehat{\text{AD}}]$ and $[\widetilde{\text{AD}}]$ are denoted by $\hat{\mathcal{L}}^u$ and $\check{\mathcal{L}}^u$, respectively.

For simplicity and *without loss of generality*, we focus on case for $u = \mathbf{0}$; i.e., no node is secured by the defender in Stage 1. With further abuse of notation, for a strategy profile $(\mathbf{0}, \psi, \phi)$, we denote $x(\mathbf{0}, \psi, \phi)$ by $x(\psi, \phi)$ as the solution of NPF model. Similarly, redefine $\hat{x}(\psi, \phi)$ and $\check{x}(\psi, \phi)$. We also drop the superscript u from \mathcal{L}^u , $\hat{\mathcal{L}}^u$ and $\check{\mathcal{L}}^u$.

Following the computational approach in the literature to solve (bilevel) interdiction problems [10], [25], we define the master-problem $[\text{AD}]^{\text{a}}$ (resp. sub-problem $[\text{AD}]^{\text{d}}$) for fixed $\phi \in \Phi$ (resp. fixed $\psi \in \Psi$):

$$\begin{aligned} [\text{AD}]^{\text{a}} \quad \psi^*(\phi) &\in \operatorname{argmax}_{\psi \in \Psi} L(x(\psi, \phi)) \quad \text{s.t.} \quad (8), \\ [\text{AD}]^{\text{d}} \quad \phi^*(\psi) &\in \operatorname{argmin}_{\phi \in \Phi} L(x(\psi, \phi)) \quad \text{s.t.} \quad (8). \end{aligned}$$

Similarly, define master- and sub- problems $[\widehat{\text{AD}}]^{\text{a}}$ and $[\widehat{\text{AD}}]^{\text{d}}$ (resp. $[\widetilde{\text{AD}}]^{\text{a}}$ and $[\widetilde{\text{AD}}]^{\text{d}}$) for the variants $[\widehat{\text{AD}}]$ (resp. $[\widetilde{\text{AD}}]$).

Sec. III-A focuses on bounding the optimal loss for $[\text{AD}]$ with the losses in $[\widehat{\text{AD}}]$ and $[\widetilde{\text{AD}}]$. We focus on the master- and sub- problems in § III-B and § III-C, respectively. This leads to an iterative approach in § III-D to solve the sub-games $[\text{AD}]$, $[\widehat{\text{AD}}]$, $[\widetilde{\text{AD}}]$. Figure 3 provides an outline of these results.

A. Upper and Lower Bounds on \mathcal{L}

Theorem 1. *Let (ψ^*, ϕ^*) , $(\hat{\psi}^*, \hat{\phi}^*)$ and $(\check{\psi}^*, \check{\phi}^*)$ be optimal solutions to $[\text{AD}]$, $[\widehat{\text{AD}}]$ and $[\widetilde{\text{AD}}]$, respectively; and denote the optimal losses by \mathcal{L} , $\hat{\mathcal{L}}$, $\check{\mathcal{L}}$, respectively. Then,*

$$\hat{\mathcal{L}} \leq \mathcal{L} \leq \check{\mathcal{L}} + \frac{\mu N}{2\mu + 4}. \quad (15)$$

To prove Theorem 1, we first prove a preliminary result that relates $x(\psi, \phi)$, $\hat{x}(\psi, \phi)$, and $\check{x}(\psi, \phi)$:

Proposition 1. *For a fixed strategy profile $(\psi, \phi) \in \Psi \times \Phi$,*

$$\hat{S} \leq S \leq \check{S}, \quad \hat{\nu} \geq \nu \geq \check{\nu}, \quad \hat{\ell} \leq \ell \leq \check{\ell}.$$

Hence,

$$\left. \begin{aligned} L_{VR}(\widehat{x}) &\leq L_{VR}(x) \leq L_{VR}(\check{x}) \\ L_{LC}(\widehat{x}) &= L_{LC}(x) = L_{LC}(\check{x}) \\ L_{LL}(\widehat{x}) &\leq L_{LL}(\widehat{x}) \leq L_{LL}(\check{x}) \end{aligned} \right\} \implies L(\widehat{x}) \leq L(x) \leq L(\check{x}). \quad (16)$$

Proposition 1 implies that any attack ψ that increases $\widehat{\mathcal{L}}$ in $[\widehat{AD}]$ (relative to the no attack case), also increases \mathcal{L} in $[AD]$ and $\check{\mathcal{L}}$ in $[\widehat{AD}]$, respectively. The converse need not be true, i.e., an attack that increases \mathcal{L} in $[AD]$ (resp. $\check{\mathcal{L}}$ in $[\widehat{AD}]$) need not increase $\widehat{\mathcal{L}}$ in $[\widehat{AD}]$ (resp. \mathcal{L} in $[AD]$). Similarly, any defender response ϕ that reduces $\check{\mathcal{L}}$ (resp. \mathcal{L}), also reduces \mathcal{L} (resp. $\widehat{\mathcal{L}}$). Again, the converse statements do not apply here.

Proof. The inequalities $\widehat{S} \leq S$ and $\widehat{\nu} \geq \nu$ are proved in [26].

The rest of the proof of Proposition 1 utilizes two lemmas.

Lemma 1. Consider a fixed $(\psi, \phi) \in \Psi \times \Phi$. The following holds: $sc = \widehat{sc} = \check{sc}$, $sg = \widehat{sg} = \check{sg}$, and

$$\check{S} = (1 + \epsilon)\widehat{S} \quad (17a)$$

$$\check{\nu} - \nu_0 \mathbf{1}_N = (1 + \epsilon)(\widehat{\nu} - \nu_0 \mathbf{1}_N) \quad (17b)$$

$$\forall (i, j) \in \mathcal{E} \quad \begin{cases} S_j = \sum_{k \in \Lambda_j} s_k + z_k \ell_k \\ \widehat{S}_j = \sum_{k \in \Lambda_j} s_k \end{cases} \quad (18a)$$

$$(18b)$$

$$\forall j \in \mathcal{N} \quad \begin{cases} \widehat{\nu}_j = \nu_0 - 2 \sum_{k \in \mathcal{N}} \mathbf{Re}(\bar{Z}_{jk} s_k) \\ \check{\nu}_j = \nu_0 - 2(1 + \epsilon) \sum_{k \in \mathcal{N}} \mathbf{Re}(\bar{Z}_{jk} s_k) \\ \widehat{\nu}_j = \nu_0 - 2 \sum_{k \in \mathcal{P}_j} \mathbf{Re}(\bar{z}_k \widehat{S}_k) \\ \check{\nu}_j = \nu_0 - 2 \sum_{k \in \mathcal{P}_j} \mathbf{Re}(\bar{z}_k \check{S}_k) \end{cases} \quad (19a)$$

$$(19b)$$

$$(19c)$$

$$(19d)$$

Proof. Recursively apply the power flow models (5), (6), and (12), from the root node to leaf nodes. ■

Lemma 2. For a fixed $(\psi, \phi) \in \Psi \times \Phi$,

$$\forall (i, j) \in \mathcal{E}, \quad S_j \leq \frac{\widehat{S}_j}{(1 - \epsilon_0)^{H - |\mathcal{P}_j| + 1}}. \quad (20)$$

Proof. We apply induction from leaf nodes to the root node. **Base case:** For any leaf node $k \in \mathcal{N}_L$,

$$\begin{aligned} z_k \ell_k &\stackrel{(A0)_4}{\leq} \epsilon_0 S_k \stackrel{(18a)}{=} \epsilon_0 (s_k + z_k \ell_k) \\ \therefore z_k \ell_k &\leq \frac{\epsilon_0 s_k}{1 - \epsilon_0} \stackrel{(18b)}{=} \frac{\epsilon_0 \widehat{S}_k}{1 - \epsilon_0}. \end{aligned}$$

Now, for any $j \in \mathcal{N} \setminus \mathcal{N}_L$,

$$\begin{aligned} z_j \ell_j &\stackrel{(A0)_4}{\leq} \epsilon_0 S_j \stackrel{(5a)}{=} \epsilon_0 \left[\sum_{k: (j,k) \in \mathcal{E}} S_k + s_j + z_j \ell_j \right] \\ \therefore z_j \ell_j &\leq \frac{\epsilon_0}{1 - \epsilon_0} \left[\sum_{k: (j,k) \in \mathcal{E}} S_k + s_j \right]. \end{aligned}$$

Adding $\sum S_k + s_j$ on both the sides:

$$\underbrace{\sum_{k: (j,k) \in \mathcal{E}} S_k + s_j + z_j \ell_j}_{S_j} \leq \frac{1}{1 - \epsilon_0} \left[\sum_{k: (j,k) \in \mathcal{E}} S_k + s_j \right].$$

Inductive step: By inductive hypothesis (IH) on \mathcal{N}_j^c ,

$$\begin{aligned} S_j &\stackrel{(IH)}{\leq} \frac{1}{(1 - \epsilon_0)^{H - |\mathcal{P}_k| + 2}} \left[\sum_{k: (j,k) \in \mathcal{E}} \widehat{S}_k + s_j \right] \\ &= \frac{\widehat{S}_j}{(1 - \epsilon_0)^{H - |\mathcal{P}_j| + 1}} \quad (\because |\mathcal{P}_j| = |\mathcal{P}_k| - 1). \end{aligned}$$

■

From Lemma 2, for any $(i, j) \in \mathcal{E}$,

$$S_j \leq \frac{\widehat{S}_j}{(1 - \epsilon_0)^{H - |\mathcal{P}_j| + 1}} \leq \frac{\widehat{S}_j}{(1 - \epsilon_0)^H} = (1 + \epsilon) \widehat{S}_j \stackrel{(17a)}{=} \check{S}_j. \quad (21)$$

For nodal voltages,

$$\begin{aligned} \nu_j &\stackrel{(5b)}{=} \nu_i - 2\mathbf{Re}(\bar{z}_j S_j) + |z_j|^2 \ell_j \\ &\geq \nu_i - 2\mathbf{Re}(\bar{z}_j S_j) \\ &\stackrel{(21)}{\geq} \nu_i - 2\mathbf{Re}(\bar{z}_j \check{S}_j). \end{aligned} \quad (22)$$

Applying (22) recursively from the node j till root node:

$$\nu_j \geq \nu_0 - 2 \sum_{k \in \mathcal{P}_j} \mathbf{Re}(\bar{z}_k \check{S}_k) \stackrel{(19d)}{=} \check{\nu}_j.$$

Thus, $\widehat{S}_j \leq S_j \leq \check{S}_j$ and $\widehat{\nu}_j \geq \nu_j \geq \check{\nu}_j$. Furthermore,

$$\begin{aligned} \widehat{S}_j \leq S_j \leq \check{S}_j &\stackrel{(A0)2}{\implies} \left| \widehat{S}_j \right|^2 \leq |S_j|^2 \leq \left| \check{S}_j \right|^2 \\ \implies \frac{\left| \widehat{S}_j \right|^2}{\widehat{\nu}_j} &\leq \frac{|S_j|^2}{\nu_j} \leq \frac{\left| \check{S}_j \right|^2}{\check{\nu}_j} \implies \widehat{\ell} \leq \ell \leq \check{\ell}. \end{aligned}$$

Finally, (16) immediately follows from (9), (10), and (15). ■

Proof of Theorem 1. For any $\mathbf{x} \in \mathcal{X}$,

$$L_{LL}(\mathbf{x}) \stackrel{(5c)}{=} \sum_{(i,j) \in \mathcal{E}} \frac{r_j(P_j^2 + Q_j^2)}{\nu_i} \stackrel{(A0)1, (A0)3}{\leq} \frac{2}{\underline{\mu}} \sum_{(i,j) \in \mathcal{E}} r_j \stackrel{(A0)3}{\leq} \frac{\underline{\mu}N}{2\underline{\mu} + 4} \quad (23)$$

Hence,

$$\begin{aligned} \check{\mathcal{L}} &= \check{L}(\check{\mathbf{x}}(\check{\psi}^*, \check{\phi}^*(\check{\psi}^*))) \\ &\geq \check{L}(\check{\mathbf{x}}(\psi^*, \check{\phi}^*(\psi^*))) && \text{(by optimality of } \check{\psi}^*) \\ &\geq \check{L}(\mathbf{x}(\psi^*, \check{\phi}^*(\psi^*))) && \text{(by Proposition 1)} \\ &\stackrel{(23)}{\geq} L(\mathbf{x}(\psi^*, \check{\phi}^*(\psi^*))) - \frac{\underline{\mu}N}{2\underline{\mu} + 4} \\ &\geq L(\mathbf{x}(\psi^*, \phi^*(\psi^*))) - \frac{\underline{\mu}N}{2\underline{\mu} + 4} && \text{(by optimality of } \phi^*) \\ &= \mathcal{L} - \frac{\underline{\mu}N}{2\underline{\mu} + 4}. \end{aligned}$$

Similarly, one can show $\mathcal{L} \geq \widehat{\mathcal{L}}$. ■

Theorem 1 implies that the value of the sub-game [AD] with NPF can be lower (resp. upper) bounded by the value of $[\widehat{AD}]$ (resp. $[\check{AD}]$). Our subsequent results show that both $[\widehat{AD}]$ and $[\check{AD}]$ admit computationally efficient solutions.

B. Optimal defender response to fixed attacker strategy ψ

We consider the sub-problem [AD]^d of computing optimal defender response $\phi^*(\psi)$ for a fixed attack ψ .

The following Lemma shows that [AD]^d is a Second-Order Cone Program (SOCP), and hence, can be solved efficiently.

Lemma 3. Let $\mathcal{X}_{CPF} := \text{conv}(\mathcal{X})$ denote the set of states \mathbf{x} satisfying (2)-(4), (5a), (5b), and the relaxation of (5c):

For a fixed $\psi \in \Psi$, the problem of minimizing $L(\mathbf{x}(\psi, \phi))$ subject to $\mathbf{x} \in \mathcal{X}_{CPF}$, (8b), (8c) is a SOCP. Its optimal solution, $\phi^{**}(\psi)$, is also optimal for [AD]^d.

For fixed ψ (attack) and fixed load control parameter γ (e.g. when changing γ is not allowed), the following proposition provides a range of optimal defender set-points $\widehat{\text{sp}}^{d*}$ and $\check{\text{sp}}^{d*}$ for LPF and ϵ -LPF models, respectively. Note that, if γ is fixed, $L_{LC}(\widehat{\mathbf{x}})$ is also fixed. Then, the defender set-points can be chosen by using $L_{VR}(\widehat{\mathbf{x}})$ as a loss function, instead of $\widehat{L}(\widehat{\mathbf{x}})$. Similar argument holds for $\check{L}(\check{\mathbf{x}})$.

Proposition 2. Consider $[\widehat{AD}]^d$ with fixed $\gamma \in \Gamma$. Then $\forall i \in \mathcal{N}$,

$$\delta_i = 0 \implies \left| \widehat{\text{sp}}_i^{d*} \right| = \overline{\text{sp}}_i, \quad \angle \widehat{\text{sp}}_i^{d*} \in [\text{arccot } \overline{K}, \text{arccot } \underline{K}].$$

Furthermore, if the DN has identical $\mathbf{r}/\mathbf{x} \equiv K$ ratio, then

$$\delta_i = 0 \implies \left| \widehat{\text{sp}}_i^{d*} \right| = \overline{\text{sp}}_i, \quad \angle \widehat{\text{sp}}_i^{d*} = \text{arccot } K. \quad (24)$$

Similar results hold for $[\widetilde{\text{AD}}]^d$.

C. Optimal attack under fixed defender response ϕ

Now, we focus on the master problem $[\text{AD}]^a$, i.e., the problem of computing optimal attack for a fixed defender response ϕ . The following Theorem characterizes the optimal attacker set-point be denoted $\text{sp}_i^{a*} = \mathbf{Re}(\text{sp}_i^{a*}) + \mathbf{jIm}(\text{sp}_i^{a*})$, when $\delta_i^* = 1$ (i.e. DER at node i is targeted by the attacker).

Theorem 2. Consider $[\text{AD}]^a$ for a fixed $\delta \in \mathcal{D}_M$ (i.e., the DERs compromised by the attacker are specified by δ and the only decision variables in $[\text{AD}]^a$ are sp^a). Then

$$\forall i \in \mathcal{N} \text{ s.t. } \delta_i = 1, \quad \text{sp}_i^{a*} = 0 - \mathbf{j}\overline{\text{sp}}_i. \quad (25)$$

Same holds for both $[\widehat{\text{AD}}]^a$ and $[\widetilde{\text{AD}}]^a$.

Proof. If $\delta_i = 1$, then $pg_i = \widehat{pg}_i = \mathbf{Re}(\text{sp}_i) = \mathbf{Re}(\text{sp}_i^{a*})$.

We first prove the simpler case for $[\widehat{\text{AD}}]^a$. From (6), one can check that as functions of \widehat{pg}_i , \widehat{P} is strictly decreasing, \widehat{Q} is constant, and $\widehat{\nu}$ is strictly increasing. Hence, $\widehat{L}(\psi, \phi_f)$ is strictly increasing in \widehat{pg}_i (because L_{VR} is non-decreasing as $\widehat{\nu}$ is decreasing; L_{LC} is constant). Hence, to minimize the loss L , the attacker chooses $\mathbf{Re}(\widehat{\text{sp}}_i^{a*}) = 0$. Similarly, $\mathbf{Im}(\widehat{\text{sp}}_i^{a*}) = -\mathbf{j}\overline{\text{sp}}_i$. Similarly, we can show that in $[\widetilde{\text{AD}}]^a$, $\widetilde{\text{sp}}^{a*} = \mathbf{0} - \mathbf{j}\overline{\text{sp}}$.

Now, we prove the case for $[\text{AD}]^a$ by contradiction. Suppose that there exists $i \in \mathcal{N}$ s.t. $\mathbf{Re}(\text{sp}_i^{a*}) > 0$. Then we can construct another attacker strategy $\widetilde{\psi}^* = [\widetilde{\delta}, \widetilde{\text{sp}}^a]$ that can further maximize L , such that $\mathbf{Re}(\text{sp}_i^{a*}) = 0$, holding all else equal, i.e., $\widetilde{\delta} = \delta, \forall j \in \mathcal{N}, \mathbf{Im}(\widetilde{\text{sp}}_j^a) = \mathbf{Im}(\text{sp}_j^{a*}), \forall j \in \mathcal{N} : j \neq i, \mathbf{Re}(\widetilde{\text{sp}}_j^a) = \mathbf{Re}(\text{sp}_j^{a*})$.

Let (sp^a, ℓ) be the decision variables for $[\text{AD}]^a$, as for fixed ϕ , the other decision variables P, Q, ν can then be written as affine functions of (sp^a, ℓ) from (5). Let (sp^{a*}, ℓ^*) (resp. $(\widetilde{\text{sp}}^a, \widetilde{\ell})$) be the solution to $[\text{AD}]^a$ when $\psi = \psi^*$ (resp. $\psi = \widetilde{\psi}$).

Let $f \in \mathbb{R}_+^N$ such that, for any $(i, j) \in \mathcal{E}$, $f_j(\text{sp}^a, \ell) := \frac{P_j^2 + Q_j^2}{\nu_i}$. Let $f^* = f(\text{sp}^{a*}, \ell^*)$, $f' = f(\widetilde{\text{sp}}^a, \ell^*)$, and $\widetilde{f} = f(\widetilde{\text{sp}}^a, \widetilde{\ell})$.

Since (sp^{a*}, ℓ^*) and $(\widetilde{\text{sp}}^a, \widetilde{\ell})$ are solutions to $[\text{AD}]^a$, they satisfy (5c). Hence, $f^* = \ell^*$, and $\widetilde{f} = \widetilde{\ell}$. Furthermore, it can be checked that $f' > f^*$. We want to show that $\widetilde{f} > f'$. Assume that $\widetilde{f} > f'$. Then, $\widetilde{f} > f^*$. Hence, $L(\widetilde{x}) > L(x^*)$, (because, $L_{\text{VR}}(\widetilde{x}) > L_{\text{VR}}(x^*)$, $L_{\text{LC}}(\widetilde{x}) = L_{\text{LC}}(x^*)$, $L_{\text{LL}}(\widetilde{x}) > L_{\text{LL}}(x)$). However, this is a contradiction, as it violates the optimality of sp^{a*} . By similar logic, we can show that $\forall i \in \mathcal{N}, \mathbf{Im}(\text{sp}_i^{a*}) = -\mathbf{j}\overline{\text{sp}}_i$.

We now prove that $\widetilde{f} > f'$, with the help of an illustrative diagram (see Figure 4).

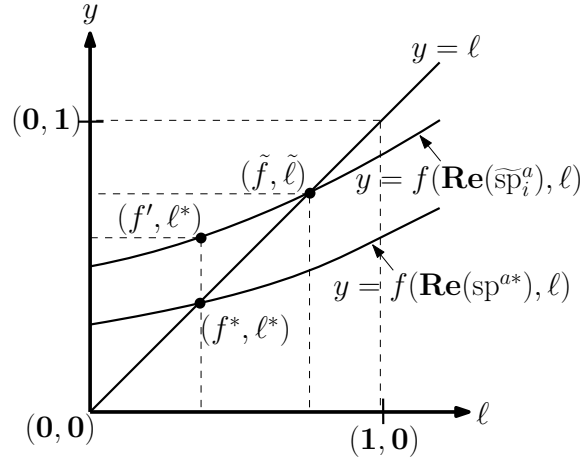


Fig. 4: Illustrative diagram showing how ℓ changes with sp^a

Note that from (5), one can show that for any ℓ , $f(\mathbf{Re}(\widetilde{\text{sp}}^a), \ell) > f(\mathbf{Re}(\text{sp}^{a*}), \ell)$. Now, consider the $(j, k)^{th}$ entry of Jacobian $\mathbf{J}_f(\ell)$.

$$\partial_{\ell_k} f_j = \frac{\nu_i (2P_j \partial_{\ell_k} P_j + 2Q_j \partial_{\ell_k} Q_j)}{\nu_i^2} - \frac{(P_j^2 + Q_j^2) \partial_{\ell_k} \nu_i}{\nu_i^2}$$

$$\begin{aligned}
\therefore 0 &\stackrel{\text{(A2)}}{\leq} \partial_{\ell_k} f_j \stackrel{\text{(A3)}}{<} \frac{(2r_k + 2x_k)}{\nu_i} + \frac{(4R_{ik}r_k + 4X_{ik}x_k)}{\nu_i^2} \\
\implies 0 &\leq \partial_{\ell_k} f_j \stackrel{\text{(A3)}}{<} (r_k + x_k) \left(\frac{2}{\mu} + \frac{4}{\mu^2} \right) \leq 1 \\
\implies 0 &\leq \hat{\partial}_{\ell_k} f_j < 1.
\end{aligned}$$

At $\ell = \mathbf{0}$, $f > \mathbf{0}$, and each entry of Jacobian $\mathbf{J}_f(\ell)$ is positive and smaller than 1. Hence, f intersects the hyper-plane $y = \ell$, exactly once. Furthermore, $f(\mathbf{Re}(\hat{\mathbf{sp}}^a, \ell)) > f(\mathbf{Re}(\mathbf{sp}^{a*}, \ell))$. Hence, we can conclude that $\tilde{\ell} = \tilde{f} > f' > f^* = \ell^*$. ■

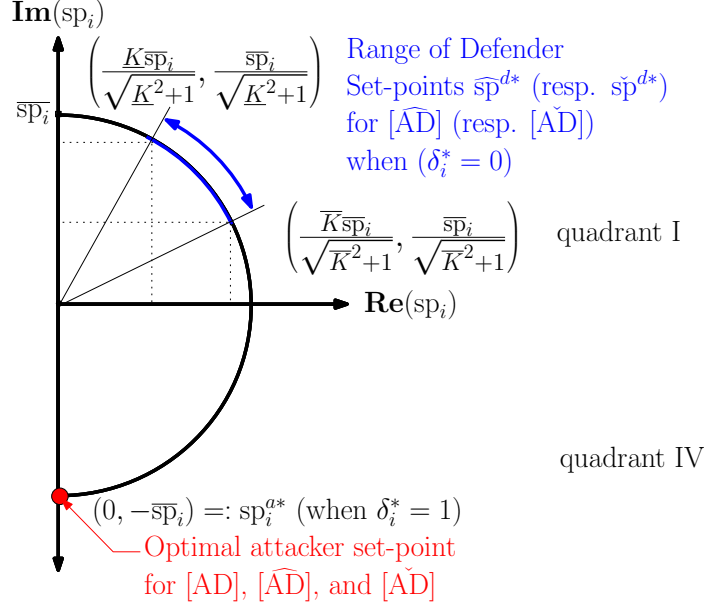


Fig. 5: Optimal attacker set-points (Theorem 2) and range for optimal defender set-points (Proposition 2).

Figure 5 shows the optimal attacker set-point \mathbf{sp}_i^{a*} for $\delta_i^* = 1$, and the defender set-points for the DERs for $\delta_j^* = 0$.

Thanks to Theorem 2, sc and sg are determined by δ and ϕ (since optimal \mathbf{sp}^{a*} is given by (25)). Thus, for given (δ, ϕ) , loss function can be denoted as $L(x(\mathbf{0} - \mathbf{j}\hat{\mathbf{sp}}, \delta), \phi)$; and [AD] can be restated as follows:

$$\mathcal{L} = \max_{\delta \in \mathcal{D}_M} \min_{\phi \in \Phi} L(x(\delta, \phi)) \quad \text{s.t.} \quad (8), (25)$$

Same holds for $[\widehat{AD}]$ (resp. $[\widetilde{AD}]$) and $[\widehat{AD}]^a$ (resp. $[\widetilde{AD}]^a$). Note that the attacker actions on DERs may not be limited to an incorrect set-point attack. For example, the attacker can simply choose to disconnect the DER nodes by choosing $\mathbf{sp}^a = \mathbf{0} + \mathbf{0j}$. However, Theorem 2 shows that the attacker will induce more loss to the defender by causing the DERs to withdraw maximum reactive power rather than simply disconnecting them.

Let $\Delta_j(\hat{\nu}_i)$ (resp. $\Delta_\delta(\hat{\nu}_i)$) be the change in voltage at node i caused due to compromise of DER at node j (resp. compromise of DERs due to attack vector δ). Similarly, define $\Delta_j(\check{\nu}_i)$ and $\Delta_\delta(\check{\nu}_i)$. We now state the following useful lemma.

Lemma 4. *If ϕ is fixed, then*

$$\forall i, j \in \mathcal{N} \begin{cases} \Delta_j(\hat{\nu}_i) = 2\mathbf{Re}(\bar{Z}_{ij}(\mathbf{sp}_j^d + \mathbf{j}\hat{\mathbf{sp}}_j)) & (26a) \\ \Delta_j(\check{\nu}_i) = 2(1 + \epsilon)\mathbf{Re}(\bar{Z}_{ij}(\mathbf{sp}_j^d + \mathbf{j}\hat{\mathbf{sp}}_j)) & (26b) \end{cases}$$

$$\forall \delta \in \mathcal{D}_M \begin{cases} \Delta_\delta(\hat{\nu}_i) = \sum_{j:\delta_j=1} \Delta_j(\hat{\nu}_i) & (27a) \\ \Delta_\delta(\check{\nu}_i) = \sum_{j:\delta_j=1} \Delta_j(\check{\nu}_i) & (27b) \end{cases}$$

For a fixed $\phi \in \Phi$, let $\hat{\mathcal{D}}_M^i(\phi)$ be the set of optimal attack vectors that maximize LPF voltage bounds violation at a pivot node, say i . Formally,

$$\hat{\mathcal{D}}_M^i(\phi) := \operatorname{argmax}_{\delta \in \mathcal{D}_M} W_i(\underline{\nu}_i - \hat{\nu}_i) \quad \text{s.t.} \quad \hat{x}(\delta, \phi) \in \hat{\mathcal{X}}, (8b), (8c) \quad (28)$$

Let $\widehat{\mathcal{D}}_M^* := \cup_{i \in \mathcal{N}} \widehat{\mathcal{D}}_M^i$, and $\widehat{\delta}^i \in \widehat{\mathcal{D}}_M^i$ denote any vector in $\widehat{\mathcal{D}}_M^i$. Similarly, define $\check{\mathcal{D}}_M^i(\phi)$, $\check{\mathcal{D}}_M^*(\phi)$, and $\check{\delta}^i$.

Using Lemma 4, Algorithm 1 computes optimal $\widehat{\delta}^*$ to maximize L_{VR} for a fixed defender action $\phi \in \Phi$ [20]. In each iteration, the Algorithm selects one node as a pivot node. For a pivot node, say i , a set of target nodes $\widehat{\delta}^i$ is determined by selecting M nodes with largest $\Delta_j(\widehat{\nu}_i)$ (see Algorithm 5 in Appendix). Applying Lemma 4, the final nodal voltage at the current pivot node i is given by $\widehat{\nu}_i - \Delta_{\widehat{\delta}^i}(\widehat{\nu}_i)$. The attack strategy that maximizes L_{VR} is the set $\widehat{\delta}^k$ corresponding to a pivot node k that admits maximum voltage bound violation when DERs specified by $\widehat{\delta}^k$ are compromised. Algorithm 1 repeatedly calls procedure Algorithm 5, considering each node as the pivot node, and hence, requires $\mathcal{O}(n^2 \log n)$ time.

Algorithm 1 Optimal Attack for Fixed Defender Response

```

1:  $\widehat{\delta}^*(\phi) \leftarrow \text{OPTIMALATTACKFORFIXEDRESPONSE}(\phi)$ 
2: procedure OPTIMALATTACKFORFIXEDRESPONSE( $\phi$ )
3:   Compute state vector for no attack  $\widehat{\mathbf{x}}(\mathbf{0}, \phi) \in \widehat{\mathcal{X}}$ 
4:   for  $i \in \mathcal{N}$  do
5:      $\widehat{\delta}^i \leftarrow \text{GETPIVOTNODEOPTIMALATTACK}(i, \text{sp}^d)$ , and calculate  $\Delta_{\widehat{\delta}^i}(\widehat{\nu}_i)$  using Lemma. 4
6:     Calculate new voltage value  $\widehat{\nu}'_i \leftarrow \widehat{\nu}_i - \Delta_{\widehat{\delta}^i}(\widehat{\nu}_i)$ 
7:   end for
8:    $k \leftarrow \text{argmax}_{i \in \mathcal{N}} W_i(\underline{\nu}_i - \widehat{\nu}'_i)$ 
9:   return  $\widehat{\delta} \leftarrow \widehat{\delta}^k$  (Pick  $\widehat{\delta}^k$  which maximally violates (1))
10: end procedure
11: procedure GETPIVOTNODEOPTIMALATTACK( $i, \text{sp}^d$ )
12:    $(J, \mathcal{N}_{g^i}, m') \leftarrow \text{OPTIMALATTACKHELPER}(i, \text{sp}^d)$ 
13:   Randomly choose  $M - m'$  nodes from  $\mathcal{N}_{g^i}$  to form  $\mathcal{N}'$ 
14:   return  $\widehat{\delta}^i \in \mathcal{D}_M$  such that  $\widehat{\delta}_k^i = 1 \iff k \in J \cup \mathcal{N}'$ 
15: end procedure

```

The following proposition shows that Algorithm 1 is optimal for DNs with identical \mathbf{r}/\mathbf{x} ratio.

Proposition 3. For a fixed $\phi \in \Phi$, let $\widehat{\delta}$ be the optimal attack vector computed by Algorithm 1. Then $\widehat{\delta}$ is also an optimal solution of $[\widehat{\text{AD}}]^a$. Same holds for $[\widetilde{\text{AD}}]^a$.

Proof. Note that for fixed $\phi \in \Phi$, maximizing $\widehat{L}(\widehat{\delta}, \phi)$ (resp. $\check{L}(\check{\delta}, \phi)$) is equivalent to maximizing $L_{\text{VR}}(\widehat{\delta}, \phi)$ (resp. $L_{\text{VR}}(\check{\delta}, \phi)$). Let $\widehat{\delta}^*$ be the optimal solution to $[\widehat{\text{AD}}]^a$.

Case (i). $L_{\text{VR}}(\widehat{\delta}^*, \phi) = 0$. Then Algorithm 1 computes $\widehat{\delta}^*$ trivially, because $0 = L_{\text{VR}}(\widehat{\delta}^*, \phi) \geq L_{\text{VR}}(\widehat{\delta}, \phi) \geq 0$. Hence, $L_{\text{VR}}(\widehat{\delta}, \phi) = L_{\text{VR}}(\widehat{\delta}^*, \phi) = 0$.

Case (ii). $L_{\text{VR}}(\widehat{\delta}^*, \phi) > 0$. Let $\widehat{\nu}_j(\delta, \phi)$ denote the nodal voltage at node j after the attack δ . Since, $\widehat{\delta} = \widehat{\delta}^k$, for some pivot node $k \in \mathcal{N}$ (see Algorithm 1), $\widehat{\delta}^k$ maximally violates (1) over all $\widehat{\delta}^i$, i.e.,

$$\forall i \in \mathcal{N}, \quad \underline{\nu}_k - \widehat{\nu}_k(\widehat{\delta}^k, \phi) \geq \underline{\nu}_i - \widehat{\nu}_i(\widehat{\delta}^i, \phi), \quad (29)$$

where $\widehat{\delta}^i$ is the optimal pivot node attack as computed by Algorithm 1 for node i , i.e.,

$$\forall i \in \mathcal{N}, \quad \forall \delta \in \mathcal{D}_M \quad \underline{\nu}_i - \widehat{\nu}_i(\widehat{\delta}^i, \phi) \geq \underline{\nu}_i - \widehat{\nu}_i(\delta, \phi). \quad (30)$$

Let $i = \text{argmax}_{j \in \mathcal{N}} W_j(\underline{\nu}_j - \widehat{\nu}_j(\widehat{\delta}^*, \phi))_+$. Furthermore, since $L_{\text{VR}}(\widehat{\delta}^*, \phi) > 0$,

$$L_{\text{VR}}(\widehat{\delta}^*, \phi) = W_i(\underline{\nu}_i - \widehat{\nu}_i(\widehat{\delta}^*, \phi)) \quad (31)$$

$$\begin{aligned} \therefore L_{\text{VR}}(\widehat{\mathbf{x}}(\widehat{\delta}, \phi)) &= L_{\text{VR}}(\widehat{\mathbf{x}}(\widehat{\delta}^k, \phi)) \\ &\stackrel{(10a)}{=} \max_{j \in \mathcal{N}} W_j(\underline{\nu}_j - \widehat{\nu}_j(\widehat{\delta}^k, \phi))_+ && \stackrel{(29)}{\geq} W_i(\underline{\nu}_i - \widehat{\nu}_i(\widehat{\delta}^i, \phi)) \\ &\stackrel{(30)}{\geq} W_i(\underline{\nu}_i - \widehat{\nu}_i(\widehat{\delta}^*, \phi)) && \stackrel{(31)}{=} L_{\text{VR}}(\widehat{\mathbf{x}}(\widehat{\delta}^*, \phi)). \end{aligned}$$

Furthermore, for a fixed ϕ $L_{\text{LC}}(\widehat{\mathbf{x}}(\widehat{\delta}, \phi)) = L_{\text{LC}}(\widehat{\mathbf{x}}(\widehat{\delta}^*, \phi))$. Hence, $\widehat{L}(\widehat{\mathbf{x}}(\widehat{\delta}, \phi)) \geq \widehat{L}(\widehat{\mathbf{x}}(\widehat{\delta}^*, \phi))$. ■

We now show that the effect of DER compromise at either node j or k on the node i depends upon the locations of nodes j and k relative to node i . The following Proposition states that if node j is upstream to node k relative to the pivot node i ($j <_i k$), then the DER compromise at node k impacts on $\widehat{\nu}_i$ more than the DER compromise on node j ; and if $j =_i k$, then the effect of DER compromise at j, k on $\widehat{\nu}_i$ is identical.

Proposition 4. [20] Consider $[\widehat{\text{AD}}]^a$. Let nodes $i, j, k \in \mathcal{N}$ where i is the pivot node, $\text{sp}_j^d = \text{sp}_k^d$, and $\overline{\text{sp}}_j = \overline{\text{sp}}_k$. If $j <_i k$ (resp. $j =_i k$), then $\Delta_j(\widehat{\nu}_i) < \Delta_k(\widehat{\nu}_i)$ (resp. $\Delta_j(\widehat{\nu}_i) = \Delta_k(\widehat{\nu}_i)$).

Same holds true for $[\widetilde{\text{AD}}]^a$.

Proposition 4 implies that, broadly speaking, compromising downstream DERs is advantageous to the attacker than compromising the upstream DERs. The following illustrative example suggests that compromising DERs by means of clustered attacks are more beneficial to the attacker than distributed attacks.

Example 1. Consider the $[\widehat{\text{AD}}]^a$ with $M = 2$ instantiated on the DN in Figure 2. Assume that all loads and DERs are homogeneous, all lines have equal impedances, i.e., $\forall i \in \mathcal{N}, sc_i = sc_a, \text{sp}_i^d = \text{sp}_a^d, \overline{\text{sp}}_i = \overline{\text{sp}}_a, z_i = z_a$. By Proposition 2, the outputs of all the DERs are fixed and identical to each other.

Let $\alpha = 2(\mathbf{Re}(\bar{z}_a(sc_a - \text{sp}_a^d)))$, and $\beta = 2(\mathbf{Re}(\bar{z}_a(\mathbf{Re}(\text{sp}_a^d) + \mathbf{j}(\mathbf{Im}(\text{sp}_a^d) + \overline{\text{sp}}_a))))$. Then ν values for different attack vectors are given in Table I. The optimal attack compromises nodes i and m , which is a cluster attack.

| Attacked Nodes | ν_m | ν_j | ν_k |
|----------------|-----------------------------|-----------------------------|-----------------------------|
| \emptyset | $\nu_0 - 23\alpha$ | $\nu_0 - 13\alpha$ | $\nu_0 - 40\alpha$ |
| $\{i, m\}$ | $\nu_0 - 23\alpha - 9\beta$ | $\nu_0 - 13\alpha - 2\beta$ | $\nu_0 - 20\alpha - 4\beta$ |
| $\{j, m\}$ | $\nu_0 - 23\alpha - 6\beta$ | $\nu_0 - 13\alpha - 4\beta$ | $\nu_0 - 20\alpha - 3\beta$ |
| $\{k, m\}$ | $\nu_0 - 23\alpha - 7\beta$ | $\nu_0 - 13\alpha - 2\beta$ | $\nu_0 - 20\alpha - 6\beta$ |
| $\{g, j\}$ | $\nu_0 - 23\alpha - 2\beta$ | $\nu_0 - 13\alpha - 5\beta$ | $\nu_0 - 20\alpha - 2\beta$ |
| $\{d, k\}$ | $\nu_0 - 23\alpha - 4\beta$ | $\nu_0 - 13\alpha - 2\beta$ | $\nu_0 - 20\alpha - 7\beta$ |

TABLE I: ν vs Different Attack Combinations

Consequently, our results (see Section IV) on security strategy in Stage 1 show that the defender should utilize his security strategy to deter cluster attacks.

D. A greedy approach for solving $[\widehat{\text{AD}}]$, $[\widetilde{\text{AD}}]$ and $[\text{AD}]$

We now utilize results for sub- and master-problems to solve $[\text{AD}]$. Consider the following assumption:

(A1) DN has identical $\mathbf{r}/\mathbf{x} \equiv K$ ratio, i.e., $\forall j \in \mathcal{N}, K_j = K$. In this subsection, we present an algorithm to solve $[\widehat{\text{AD}}]$ and $[\widetilde{\text{AD}}]$ under **(A1)**, and then propose its extension, a greedy iterative approach, for solving $[\text{AD}]$ under the general case.

Under **(A1)**, the optimal defender set-points $\widehat{\text{sp}}^{d^*}$ and $\check{\text{sp}}^{d^*}$ are as specified by Proposition 2, and hence fixed. For fixed optimal $\widehat{\text{sp}}^{d^*}$ (resp. $\check{\text{sp}}^{d^*}$), we can solve the problem $[\widehat{\text{AD}}]$ (resp. $[\widetilde{\text{AD}}]$) by using Benders Cut method [25]. However, we present a computationally faster algorithm, Algorithm 2 that computes attacker's candidate optimal attack vectors $\widehat{\mathcal{D}}_M^*$ (resp. $\check{\mathcal{D}}_M^*$) using Lemma 4.

Lemma 5. Under **(A0)**, **(A1)**, for any two fixed $\widehat{\gamma}^1, \widehat{\gamma}^2 \in \Gamma$, $\widehat{\mathcal{D}}_M^*(\widehat{\text{sp}}^{d^*}, \widehat{\gamma}^1) = \widehat{\mathcal{D}}_M^*(\widehat{\text{sp}}^{d^*}, \widehat{\gamma}^2)$.

Given $\widehat{\text{sp}}^d \in \mathcal{S}$, it can be checked that Algorithm 2, in fact, computes $\widehat{\mathcal{D}}_M^i(\widehat{\text{sp}}^d)$, and $\widehat{\mathcal{D}}_M^*(\widehat{\text{sp}}^d) = \bigcup_{i \in \mathcal{N}} \widehat{\mathcal{D}}_M^i(\widehat{\text{sp}}^d)$ is the set of candidate optimal attack vectors. The cardinality of the set $\widehat{\mathcal{D}}_M^i$ (Line 4) in the worst-case can be as high as $\mathcal{O}(e^{\frac{n}{e}})$. Therefore, computing $\widehat{\mathcal{D}}_M^*$ can take $\mathcal{O}(ne^{\frac{n}{e}})$ time in the worst-case.

Algorithm 2 computes the set of attacks $\widehat{\mathcal{D}}_M^*(\widehat{\text{sp}}^{d^*})$, and iterates over each $\widehat{\delta} \in \widehat{\mathcal{D}}_M^*(\widehat{\text{sp}}^{d^*})$. In each iteration, since $\text{sp}^d = \widehat{\text{sp}}^{d^*}$ is fixed, the sub-problem $[\widehat{\text{AD}}]^d$ reduces to an LP over the variable γ . Let $\widehat{\gamma}^*(\widehat{\delta})$ be the solution to the LP. Then, $\widehat{\phi}^*(\widehat{\delta}) = [\widehat{\text{sp}}^{d^*}, \widehat{\gamma}^*(\widehat{\delta})]$ is the optimal solution to $[\widehat{\text{AD}}]^d$. Choosing $\widehat{\delta}^* = \arg\max_{\widehat{\delta} \in \widehat{\mathcal{D}}_M^*} L(\widehat{x}(\widehat{\delta}, \widehat{\phi}^*(\widehat{\delta})))$, Algorithm 2 computes the solution to be $(\widehat{\delta}^*, \widehat{\phi}^*(\widehat{\delta}^*))$ to the problem $[\widehat{\text{AD}}]$. Similarly, we can use Algorithm 2 to solve $[\widetilde{\text{AD}}]$.

Theorem 3. Under **(A0)**, **(A1)**, let $(\widehat{\delta}, \widehat{\phi})$ be a solution computed by Algorithm 2. Then $(\widehat{\delta}, \widehat{\phi})$ is also an optimal solution to $[\widehat{\text{AD}}]$. Similar result holds for $[\widetilde{\text{AD}}]$.

Proof. Under **(A1)**, $\text{sp}^d = \widehat{\text{sp}}^{d^*}$ is fixed (Proposition 2). Then, for any $\gamma \in \Gamma$, by Lemma 5 and Proposition 3, the optimal attack $\widehat{\delta}^*$ belongs to the set $\widehat{\mathcal{D}}_M^*(\widehat{\text{sp}}^{d^*})$. Algorithm 2 iterates over the attack vectors $\delta \in \widehat{\mathcal{D}}_M^*$, computes $\widehat{\gamma}^*(\delta)$ by solving an LP, and calculates the loss $\widehat{L}(\widehat{x}(\delta, \widehat{\phi}^*(\delta)))$. Finally, it returns the solution corresponding to the maximum loss. Similarly, Algorithm 2 also computes optimal solution for $[\widetilde{\text{AD}}]$. ■

Proposition 5. Under **(A0)**, **(A1)**, $\widehat{\mathcal{D}}_M^*(\widehat{\text{sp}}^{d^*}) = \check{\mathcal{D}}_M^*(\check{\text{sp}}^{d^*})$.

Algorithm 2 Solution to $[\widehat{\text{AD}}]$ for DNs with identical \mathbf{r}/\mathbf{x}

```

1:  $(\hat{\delta}^*, \hat{\phi}^*, \hat{\mathcal{L}}) \leftarrow \text{GREEDY-ONE-SHOT}()$ 
2: procedure GREEDY-ONE-SHOT()
3:    $\hat{\mathcal{L}} = 0, \hat{\delta}^* = \mathbf{0}, \hat{\gamma}^* = \mathbf{1}, \hat{\text{sp}}^{\text{d}^*}$  as in Proposition 2
4:   Let  $\hat{\mathcal{D}}_M^i = \text{GETPIVOTNODEOPTIMALATTACKSET}(i, \hat{\text{sp}}^{\text{d}^*})$ 
5:    $\hat{\mathcal{D}}_M^* = \bigcup_{i \in \mathcal{N}} \hat{\mathcal{D}}_M^i$ 
6:   For each  $\delta \in \hat{\mathcal{D}}_M^*$ , compute  $\hat{\gamma}^*(\delta)$  by solving  $[\widehat{\text{AD}}]^{\text{d}}$  as an LP in  $\gamma$ . Let  $\hat{\phi}^*(\delta) = \hat{\text{sp}}^{\text{d}^*}, \hat{\gamma}^*(\delta)$ 
7:   Let  $\hat{\delta}^* := \underset{\delta \in \hat{\mathcal{D}}_M^*}{\text{argmax}} \hat{\mathcal{L}}(\hat{\mathbf{x}}(\delta), \hat{\gamma}^*(\delta), \hat{\text{sp}}^{\text{d}^*})$ 
8:   return  $\hat{\delta}^*, \hat{\phi}^* = \hat{\phi}^*(\hat{\delta}^*), \hat{\mathcal{L}} = \hat{\mathcal{L}}(\hat{\mathbf{x}}(\hat{\delta}^*), \hat{\phi}^*)$ 
9: end procedure
10: procedure GETPIVOTNODEOPTIMALATTACKSET( $i, \text{sp}^{\text{d}}$ )
11:    $(J, \mathcal{N}_{g^i}, m') \leftarrow \text{OPTIMALATTACKHELPER}(i, \text{sp}^{\text{d}})$ 
12:   return  $\mathcal{D}_M^i \leftarrow \{\delta \in \mathcal{D}_M \mid \delta_k = 1 \text{ iff } k \in J \cup \mathcal{N}', \text{ where } \mathcal{N}' \subseteq \mathcal{N}_{g^i} \text{ and } |\mathcal{N}'| = M - m'\}$ 
13: end procedure

```

Proof. Under (A1), the DER set-points are as specified by Proposition 2. Hence, $\hat{\text{sp}}^{\text{d}^*} = \check{\text{sp}}^{\text{d}^*}$. Furthermore, $\forall j \in \mathcal{N}, \Delta_j(\check{\nu}_i) = (1 + \epsilon)\Delta_j(\nu_i)$. Hence, the sequence of partitions of the nodes for every pivot node is the same in both the LPF and the ϵ -LPF model. Hence, $\hat{\mathcal{D}}_M^*(\hat{\text{sp}}^{\text{d}^*}) = \check{\mathcal{D}}_M^*(\check{\text{sp}}^{\text{d}^*})$. ■

We, now, describe an iterative greedy approach to compute the solution to [AD] that uses the optimal attacker strategy for fixed defender response (refer Algorithm 1).

Algorithm 3 initializes ϕ_c to the optimal defender response under no attack. In the first step of the iterative approach, the attacker assumes some defender response ϕ_c to be fixed, and computes the optimal attack strategy $\delta_c(\phi_c)$ using the greedy Algorithm 1. Then in the second step, the defender computes a new defense strategy ϕ_c optimal for fixed δ_c by solving the SOCP, and updates the defender response. If $L(\mathbf{x}(\delta_c, \phi_c)) > L(\mathbf{x}(\delta^*, \phi^*))$, then the current best solution (δ^*, ϕ^*) is updated to (δ_c, ϕ_c) . Then in the next iteration, the attacker uses this new defender response to update his attack strategy, and so on and so forth. If this δ_c has already been discovered in some previous iteration, the algorithm terminates successfully, with δ^*, ϕ^* as the required optimal attack plan, and the corresponding optimal defense. The algorithm terminates unsuccessfully if the number of iterations exceeds a maximum limit.

Algorithm 3 Iterative Algorithm for Greedy Approach

```

1:  $(\delta^*, \phi^*, \mathcal{L}) \leftarrow \text{GREEDY-ITERATIVE}()$ 
2: procedure GREEDY-ITERATIVE
3:   Let  $\delta^* \leftarrow \mathbf{0}, \mathcal{L}^* \leftarrow 0, \delta_c \leftarrow \mathbf{0}, \text{iter} \leftarrow 0, \Upsilon \leftarrow \emptyset, \phi_c, \phi^*, \Upsilon$ 
4:   For  $\delta = \delta_c$  compute  $\phi^*$  by solving SOCP  $[\text{AD}]^{\text{d}}$  (Lem. 3)
5:    $\phi_c \leftarrow \phi^*, \mathcal{L}^* \leftarrow L(\check{\mathbf{x}}(\delta, \phi^*))$ 
6:   for  $\text{iter} \leftarrow 0, 1, \dots, \text{maxIter}$  do
7:      $\delta_c \leftarrow \text{OPTIMALATTACKFORFIXEDRESPONSE}(\phi_c)$ 
8:     // If  $\delta_c$  previously found, successfully terminate
9:     if  $\delta_c \in \Upsilon$  then return  $\delta^*, \phi^*$ 
10:    else  $\Upsilon = \Upsilon \cup \{\delta_c\}$  // Store the current best attack vector
11:    Compute  $\phi_c$  by solving SOCP  $[\text{AD}]^{\text{d}}$  Lem. 3
12:    if  $L(\check{\mathbf{x}}(\delta_c, \phi_c)) > \mathcal{L}^*$  then
13:       $\delta^* \leftarrow \delta_c, \phi^* \leftarrow \phi_c, \mathcal{L}^* \leftarrow L(\check{\mathbf{x}}(\delta, \phi^*))$ 
14:    end if
15:  end for // Maximum Iteration Limit reached
16:  Return  $\delta^*, \phi^*, \mathcal{L}^*$  // Return the last best solution
17: end procedure // Algo terminates unsuccessfully

```

Note that in each iteration, the size of Υ increases by 1, hence, the algorithm is bound to terminate after exhausting all possible attack vectors.

Proposition 5 and Theorem 3 can be applied for any $u \in \mathcal{U}_B$, since if the DN has identical \mathbf{r}/\mathbf{x} ratio, sp^{d} are also fixed.

The following proposition states that for a fixed defender action ϕ , the optimal attack solutions obtained by $[\widehat{\text{AD}}]^{\text{a}}$ and

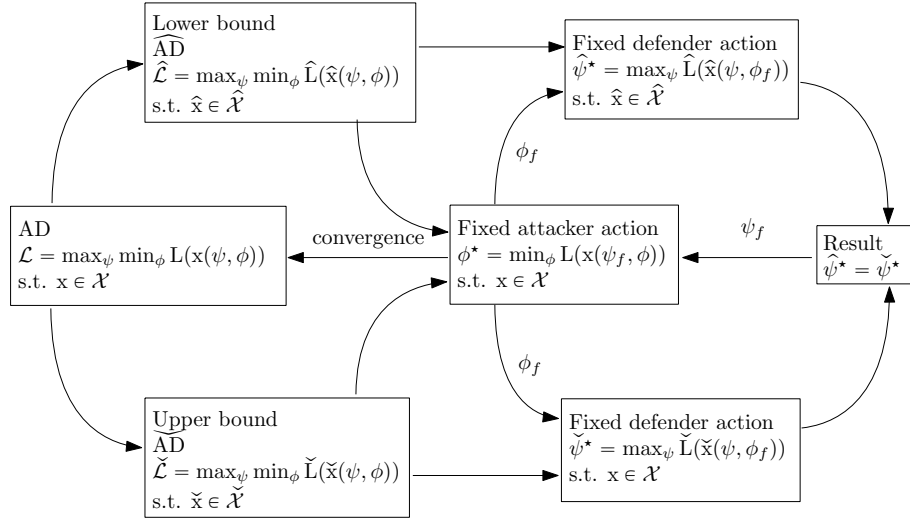


Fig. 6: Overall Computational Approach

$[\widehat{\text{AD}}]^a$ are identical.

Proposition 6. Assume that $\underline{\nu}_i = \underline{\nu}_j = \underline{\nu}$ and $W_i = W_j = W \forall i, j \in \mathcal{N}$. For a fixed defender action ϕ , let the optimal attack as computed under $[\widehat{\text{AD}}]^a$ and $[\check{\text{AD}}]^a$ be denoted by $\widehat{\psi}^*(\phi)$ and $\check{\psi}^*(\phi)$, respectively, such that

$$L_{\text{VR}}(\widehat{x}(\widehat{\psi}^*, \phi)) > 0 \quad \text{and} \quad L_{\text{VR}}(\check{x}(\check{\psi}^*, \phi)) > 0. \quad (32)$$

Then,

$$\widehat{\psi}^* \in \operatorname{argmax}_{\psi \in \Psi} \check{\mathcal{L}}(\check{x}(\psi, \phi)) \quad \text{s.t.} \quad \check{x} \in \check{\mathcal{X}} \quad (33a)$$

$$\check{\psi}^* \in \operatorname{argmax}_{\psi \in \Psi} \widehat{\mathcal{L}}(\widehat{x}(\psi, \phi)) \quad \text{s.t.} \quad \widehat{x} \in \widehat{\mathcal{X}} \quad (33b)$$

Proof. For fixed defender action ϕ , and for any $\psi_1, \psi_2 \in \Psi$,

$$L_{\text{LC}}(\widehat{x}(\psi_1, \phi)) = L_{\text{LC}}(\widehat{x}(\psi_2, \phi)) \quad \text{and} \quad (34)$$

$$L_{\text{LC}}(\check{x}(\psi_1, \phi)) = L_{\text{LC}}(\check{x}(\psi_2, \phi)). \quad (35)$$

Suppose $\widehat{\psi}^*$ is not an optimal solution to $[\widehat{\text{AD}}]^a$. Then,

$$\begin{aligned} \check{\mathcal{L}}(\check{x}(\check{\psi}^*, \phi)) &> \check{\mathcal{L}}(\check{x}(\widehat{\psi}^*, \phi)) \\ \stackrel{(35)}{\iff} L_{\text{VR}}(\check{x}(\check{\psi}^*, \phi)) &> L_{\text{VR}}(\check{x}(\widehat{\psi}^*, \phi)) \\ \iff \max_{i \in \mathcal{N}} W_i(\underline{\nu}_i - \check{\nu}_i(\check{\psi}^*, \phi))_+ &> \max_{j \in \mathcal{N}} W_j(\underline{\nu}_j - \check{\nu}_j(\widehat{\psi}^*, \phi))_+ \\ \stackrel{(32)}{\iff} \max_{i \in \mathcal{N}} (\underline{\nu} - \check{\nu}_i(\check{\psi}^*, \phi)) &> \max_{j \in \mathcal{N}} (\underline{\nu} - \check{\nu}_j(\widehat{\psi}^*, \phi)) \\ \iff \max_{i \in \mathcal{N}} (\nu_0 - \check{\nu}_i(\check{\psi}^*, \phi)) &> \max_{j \in \mathcal{N}} (\nu_0 - \check{\nu}_j(\widehat{\psi}^*, \phi)) \\ \stackrel{(17b)}{\iff} (1 + \epsilon) \left\| (\nu_0 - \widehat{\nu}_i(\check{\psi}^*, \phi)) \right\|_{\infty} &> (1 + \epsilon) \left\| (\nu_0 - \widehat{\nu}_j(\widehat{\psi}^*, \phi)) \right\|_{\infty} \\ \stackrel{(32)}{\iff} \max_{i \in \mathcal{N}} W_i(\underline{\nu}_i - \widehat{\nu}_i(\check{\psi}^*, \phi))_+ &> \max_{j \in \mathcal{N}} W_j(\underline{\nu}_j - \widehat{\nu}_j(\widehat{\psi}^*, \phi))_+ \\ \iff L_{\text{VR}}(\widehat{x}(\check{\psi}^*, \phi)) &> L_{\text{VR}}(\widehat{x}(\widehat{\psi}^*, \phi)) \\ \stackrel{(35)}{\iff} \widehat{\mathcal{L}}(\widehat{x}(\check{\psi}^*, \phi)) &> \widehat{\mathcal{L}}(\widehat{x}(\widehat{\psi}^*, \phi)). \end{aligned}$$

Hence, the contradiction that $\widehat{\psi}^*$ is an optimal solution to $[\widehat{\text{AD}}]^a$. Similarly, we can show that $\check{\psi}^*$ is an optimal solution to $[\check{\text{AD}}]^a$. \blacksquare

Our overall computational approach to solving the problem $[\text{AD}]$, thus far, can be summarized as in Figure 6. Given an instance of the problem $[\text{AD}]$, we first solve the problems $[\widehat{\text{AD}}]$ and $[\check{\text{AD}}]$. For this, we employ an iterative procedure that

iterates between the master- and sub- problems. For a fixed attacker action we determine the optimal defender response ϕ for the $[\text{AD}]^d$ using the convex relaxation of (5c). Then, for the fixed defender response ϕ , we compute the optimal attacker strategies $\hat{\psi}^*$ and $\check{\psi}^*$ by solving $[\text{AD}]^a$ and $[\text{AD}]^a$, respectively. Proposition 6 provides us an useful result that $\psi^*(\phi) := \hat{\psi}^* = \check{\psi}^*$. This optimal attacker strategy $\psi^*(\phi)$ is then fed back to the master- problem $[\text{AD}]^a$. This procedure is repeated until we reach a convergence or we exceed the maximum iteration limit.

IV. SECURING DERS TO WORST-CASE ATTACKS

In this section, we consider the defender problem of optimal security investment in Stage 1. For simplicity, we restrict our attention to DNs that satisfy the following assumption:

(A2) Symmetric Network. For every $i \in \mathcal{N}$, for any two nodes $j, k \in \mathcal{N}_i^c$, Λ_j and Λ_k are symmetrically identical about node i . That is, $z_j = z_k$, $|\mathcal{N}_j^c| = |\mathcal{N}_k^c|$, $sc_j^{\text{nom}} = sc_k^{\text{nom}}$, $\underline{\nu}_j = \underline{\nu}_k$, $W_j = W_k$, and $C_j = C_k$. However, all the DERS are homogeneous, i.e., $\forall j, k \in \mathcal{N}$, $\overline{sp}_j = \overline{sp}_k$.

Let B be a fixed security budget. Let $u, \tilde{u} \in \mathcal{U}_B$, $u \neq \tilde{u}$, be two security strategies. Strategy u is *more secure* than strategy \tilde{u} (denoted by $u \leq \tilde{u}$) under NPF (resp. LPF), if $\mathcal{L}^u \leq \mathcal{L}^{\tilde{u}}$ (resp. $\hat{\mathcal{L}}^u \leq \hat{\mathcal{L}}^{\tilde{u}}$). Finally, we ask what is the best security strategy u^* , such that for $u = u^*$, \mathcal{L}^u is minimized. Figure 7 shows two possible security strategies u^1 (Figure 7a) and u^2 (Figure 7b). If we compare u^1 and u^2 , while transitioning from u^1 to strategy u^2 , 3 secure nodes in Λ_2 subtree go up a level each, while 3 secure nodes in Λ_3 subtree go down a level each. Then, between u^1 and u^2 , which strategy is more secure? In this section, we provide insights about optimal security strategies under **(A2)**, which help show that u^2 is more secure than u^1 .

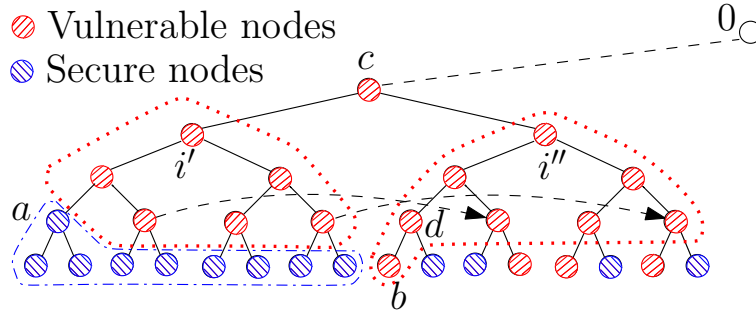
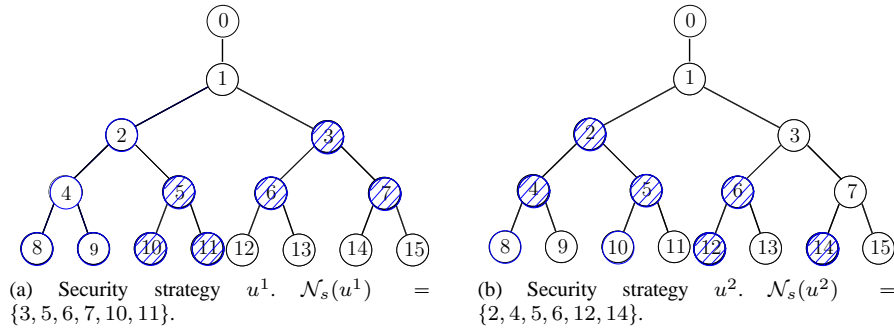


Fig. 7: Different defender security strategies.

Algorithm 4 computes an optimal security strategy $[\widehat{\text{DAD}}]$ under **(A0)-(A2)**. It initially assigns all nodes to be vulnerable. Then, DER nodes are secured sequentially in a bottom-up manner towards the root node. If the security budget is not adequate to secure a full level, the nodes in that level are uniformly secured and the remaining nodes are not secured. Under all the assumptions of Algorithm 4, it takes $\mathcal{O}(n)$ time.

In the following theorem, we show that the security strategy computed by Algorithm 4 is an optimal solution to the Stage 1 of $[\widehat{\text{DAD}}]$ problem.

Theorem 4. Assume **(A0)**, **(A1)**, **(A2)**. Let \hat{u}^* be the security strategy computed by Algorithm 4. Furthermore, with $u = \hat{u}^*$, let $(\hat{\psi}^*, \hat{\phi}^*)$ be the solution computed by Algorithm 2. Then, $(\hat{u}^*, \hat{\psi}^*, \hat{\phi}^*)$ is an optimal solution to $[\widehat{\text{DAD}}]$. Similar result holds for $[\text{DAD}]$.

Consider any security strategy $u \in \mathcal{U}_B$ such that

$$u = \begin{bmatrix} \frac{u_1}{1} & \frac{u_2}{2} & \cdots & \frac{1}{a} & \cdots & \frac{0}{b} & \cdots & \frac{u_N}{N} \end{bmatrix}. \quad (36)$$

Construct \tilde{u} from u by only flipping the bits at nodes a and b as follows:

$$\tilde{u} = \begin{bmatrix} \frac{u_1}{1} & \frac{u_2}{2} & \cdots & \frac{0}{a} & \cdots & \frac{1}{b} & \cdots & \frac{u_N}{N} \end{bmatrix}, \quad (37)$$

i.e., $\tilde{u}_i = u_i \quad \forall \quad i \in \mathcal{N} \setminus \{a, b\}$. Similarly, let $\delta \in \mathcal{D}_M(u)$ such that $\delta_a = 0, \delta_b = 1$; and construct $\tilde{\delta}$ from δ as in (37) such that $\tilde{\delta}_i = \delta_i \quad \forall \quad i \in \mathcal{N} \setminus \{a, b\}$. Note that, $\tilde{\delta} \in \mathcal{D}_M(\tilde{u})$.

Algorithm 4 Optimal security strategy

```

1:  $\hat{u}^* \leftarrow \text{OPTIMALSECURITYSTRATEGY}()$ 
2: procedure OPTIMALSECURITYSTRATEGY()
3:    $n_s \leftarrow 0, h \leftarrow H, \hat{u} \leftarrow \mathbf{0}$  // Initialize all nodes to vulnerable nodes
4:   For each  $h \in [1, 2, \dots, H]$ , let  $\alpha_h \leftarrow \sum_{j=h}^H |\mathcal{N}_j|$ 
5:   Let  $h' \leftarrow \operatorname{argmax}_{h \in [1, \dots, H]: \alpha_h \geq M} h$ 
6:   Let  $\forall h \in [h', \dots, H], \forall i \in \mathcal{N}'_h, \hat{u}_i \leftarrow 1$ .
7:   Let  $\mathcal{N}'_{h'} \subseteq \mathcal{N}_{h'}$  be a set of uniformly chosen  $M - \alpha_{h'+1}$  nodes on level  $h'$ .
8:   For each  $i \in \mathcal{N}'_{h'}, \hat{u}_i \leftarrow 1$ 
9:   return  $\hat{u}$ 
10: end procedure

```

To prove Theorem 4, we introduce the following sequence of propositions, where we compare the security strategies u and \tilde{u} under various conditions.

Proposition 7. Assume (A0), (A1), (A2). Let $u \in \mathcal{U}_B$ (resp. $\tilde{u} \in \mathcal{U}_B$) be as in (36) (resp. (37)). If $b \in \Lambda_a$, then $u \preceq \tilde{u}$.

Starting with any strategy $u' \in \mathcal{U}_B$, Proposition 7 can be applied recursively to obtain a more secure strategy $u \in \mathcal{U}_B : u' \preceq u$, which has the property that if a node i is secure, then all its successor nodes (i.e. all nodes in subtree Λ_i) are also secured by the defender, i.e.,

$$\forall i \in \mathcal{N}, u_i = 1 \implies \forall j \in \Lambda_i, u_j = 1 \quad (38)$$

Proposition 8. Assume (A0), (A1), (A2). Let $u \in \mathcal{U}_B$ (resp. $\tilde{u} \in \mathcal{U}_B$) be as in (36) (resp. (37)). Let $A_u = \{(i, j) \in \mathcal{N} \times \mathcal{N} \mid u_i = 1, u_j = 0, h_i \geq h_j + 1\}$. If u satisfies (38), and $(a, b) \in \operatorname{argmax}_{(i, j) \in A_u} |\mathcal{P}_i \cap \mathcal{P}_j|$, then $u \preceq \tilde{u}$.

Again, starting with any strategy $u' \in \mathcal{U}_B$, we can apply Proposition 8 recursively to obtain a more secure strategy $u \in \mathcal{U}_B : u' \preceq u$, in which, if a node is secure, then all nodes in lower levels are also secured by the defender, i.e.,

$$\forall i, j \in \mathcal{N}, (u_i = 1 \text{ and } h_j > h_i) \implies u_j = 1 \quad (39)$$

Thus, Proposition 8 is a generalization of Proposition 7.

Proposition 9. Assume (A0), (A1), (A2). Let $u \in \mathcal{U}_B$ be such that u satisfies (39). Let $h' = \operatorname{argmin}_{(\exists a \in \mathcal{N}_h: u_a = 1)} h$. If the secure nodes on level h' are uniformly distributed over the level h' , i.e., $|\mathcal{N}_j^c \cap \mathcal{N}_s| \in \{T, T+1\}, \forall j \in \mathcal{N}_{h'}$, where $T \in \mathbb{Z}_+$, then u is an optimal security strategy, i.e., $\forall \tilde{u} \in \mathcal{U}_B, \tilde{u} \preceq u$.

Proposition 9 implies that there exists an optimal security strategy in which there is a top-most level with DER nodes that are uniformly chosen for security investment.

Proof of Theorem 4. Let $u^{*1} \in \mathcal{U}_B$ be any optimal security strategy. From u^{*1} , by sequentially applying Proposition 7, Proposition 8, and Proposition 9, we can obtain an optimal security strategy u^{*2} that satisfies (38), (39), and has the top-most level with secure nodes having uniformly distributed secured nodes.

Now, let \hat{u}^* be the output of Algorithm 4. Since in Algorithm 4, nodes are secured from the leaf nodes to the root node level-by-level, \hat{u}^* also satisfies (38) and (39). The Algorithm 4 also secures the top-most level with secure nodes with uniformly distributed secured nodes, \hat{u}^* is the same as u^{*2} upto a homomorphic transformation.

Finally, we argue that under (A0)-(A2), \hat{u}^* can be combined with previous results to obtain full solution of $[\widehat{\text{DAD}}]$. Under (A1), the defender set-points are fixed. Since, \hat{u} and $\widehat{\text{sp}}^{\text{d}^*}$ are both fixed, we can compute the set of candidate optimal attack vectors $\widehat{\mathcal{D}}_M^*$, by considering only vulnerable DERs. Then for a fixed $\delta \in \widehat{\mathcal{D}}_M^*$, the sub-problem $[\widehat{\text{AD}}]^{\text{d}}$ reduces to an LP in

γ . Hence, Algorithm 2 solves for $(\hat{\psi}^*, \hat{\phi}^*)$, the optimal solution of $[\widehat{\text{AD}}]$ for $u = \hat{u}$, by iterating over $\delta \in \widehat{\mathcal{D}}_M^*$. The strategy profile $(\hat{u}^*, \hat{\psi}^*, \hat{\phi}^*)$, thus obtained, is an optimal solution to for DNs that satisfy **(A0)**, **(A1)**, **(A2)**. Similarly, we can solve $[\widehat{\text{DAD}}]$. ■

Propositions 7 and 8 capture the attacker preference for the downstream DERs, whereas Proposition 9 capture the attacker preference for cluster attacks. Hence, the optimal security strategy has distributed secured nodes.

Let us revisit the security strategies u^1 and u^2 in Figure 7: which one is better? Firstly, we use symmetry **(A2)** to argue that securing nodes 2, 4, 5 is equivalent to securing nodes 3, 6, 7. Then, Λ_3 subtree of u^2 has more distributed secured nodes than Λ_2 in u^1 . Hence, strategy 2 is better. Theorem 4 will, of course, give the optimal security strategy \hat{u}^* in which nodes $\mathcal{N}_s(\hat{u}^*) = \{8, 9, 10, 12, 13, 14\}$, or other homomorphic strategies of \hat{u}^* .

We state without proof the following Proposition:

Proposition 10. 1) Under **(A0)**, **(A1)**, **(A2)**, any attack vector in $\widehat{\mathcal{D}}_M^*$, can be considered as a homomorphic transformation of an element of a subset of $\widehat{\mathcal{D}}_M^*$ which is at most of size $|\mathcal{N}_v| \leq N$.
2) Under **(A0)**, **(A1)**, if $\forall i, j, k \in \mathcal{N}$ such that $\overline{\text{sp}}_j > 0$ and $\overline{\text{sp}}_k > 0$, $\Delta_j(\hat{v}_i) \neq \Delta_k(\hat{v}_i)$, then $|\widehat{\mathcal{D}}_M^*| = N$.

Due to Theorem 4 and item 2, we can compute the optimal solution for $[\widehat{\text{DAD}}]$, in $\mathcal{O}(\text{poly}(N))$. Same holds for $[\widehat{\text{DAD}}]$.

Admittedly, our structural results on optimal security investment in Stage 1 of the game are specific to assumption **(A2)**. Future work involves extending these results to a general radial DN with heterogeneous DER nodes. A key aspect in effort will be to understand how the defender's net value of securing an individual DER node depends on its capacity and location in the DN.

V. COMPUTATIONAL STUDY

We describe a set of computational experiments to evaluate the performance of the iterative Greedy Approach (GA) in solving $[\text{AD}]$; see Algorithm 3. (We again assume $u = \mathbf{0}$.) We compare the optimal attack strategies and optimal defender set-points obtained from GA with the corresponding solutions obtained by conducting an exhaustive search (or Brute Force(BF)), and by implementing the Benders Cut (BC) algorithm. We refer the reader to [10], [25], for the BC algorithm adopted here⁶. The abbreviations BC-LPF and BC-NPF denote the solutions obtained by applying optimal attack strategies from $[\widehat{\text{AD}}]$ to LPF and NPF, respectively. Importantly the experiments illustrate the impact of attacker's resource (M) and defender's load control capability $\underline{\gamma}$ on the optimal value of $[\text{AD}]$. The code for this computational study can be obtained by contacting the authors.

Network Description: Our prototypical DN is a modified IEEE 37-node network; see Figure 1. We consider two variants of this network: homogeneous and heterogeneous. **Homogeneous Network** (\mathcal{G}^I) has 14 homogeneous DERs with randomly assigned node locations, loads with equal nominal demand, and lines with identical \mathbf{r}/\mathbf{x} ratio. Table II (in appendix) lists the parameter values of \mathcal{G}^I . **Heterogeneous Network** (\mathcal{G}^H) has same topology as \mathcal{G}^I , but has heterogeneous DERs (chosen at random from 3 different DER apparent power capabilities), heterogeneous loads, and lines with different \mathbf{r}/\mathbf{x} ratios. The location of DER nodes, the total nominal generation capacity, and the total nominal demand in \mathcal{G}^H is roughly similar to the corresponding values for \mathcal{G}^I .

DER output vs M. Figure 8 compares the DER output (sg) of uncompromised DERs that form part of defender response in \mathcal{G}^I and \mathcal{G}^H for different M. When $M = 0$ (no attack), there are no voltage violations, and the defender minimizes L_{LL} by producing more $pg > qg$. For $M > 0$, the voltage bounds are violated. To limit L_{VR} , the defender responds by increasing qg ; and the output of uncompromised DERs lie in a neighborhood of $\theta = \text{arccot } \mathbf{r}/\mathbf{x}$. For the case of \mathcal{G}^H (Figure 8b), the set-points of the uncompromised DERs are more spread out for voltage regulation over different \mathbf{r}/\mathbf{x} ratios (Proposition 2). In Figure 8b the three semi-circles correspond to the uncompromised DERs with different apparent power capabilities. These observations on defender response validate Proposition 2.

GA vs. BC-NPF, BC-LPF and BF. Figure 9 compares results obtained from *BC-NPF*, *GA*, and *BF* on \mathcal{G}^I . We consider two cases with the maximum controllable load percentage $\underline{\gamma} = 50\%$ and $\underline{\gamma} = 70\%$. For each case, we vary M from 0 to $|\mathcal{N}_v| = 14$; and also vary \mathbf{W}/\mathbf{C} ratios to capture the effect of different weights on the terms L_{VR} and L_{LC} .

⁶In the BC-implementation of [25], the inner sub-problem is in LP. To apply BC to $[\widehat{\text{AD}}]$, the non-linearity due to (4) is addressed by fixing the set-points according to Proposition 2. In our implementation, we choose $\widehat{\text{sp}}^{d*} = \arctan K_{avg}$, where $K_{avg} := \frac{\sum_{(i,j) \in \mathcal{E}} r_j}{\sum_{(i,j) \in \mathcal{E}} x_j}$ is the ratio of sum of resistances over all the lines to the sum of reactances over all the lines.

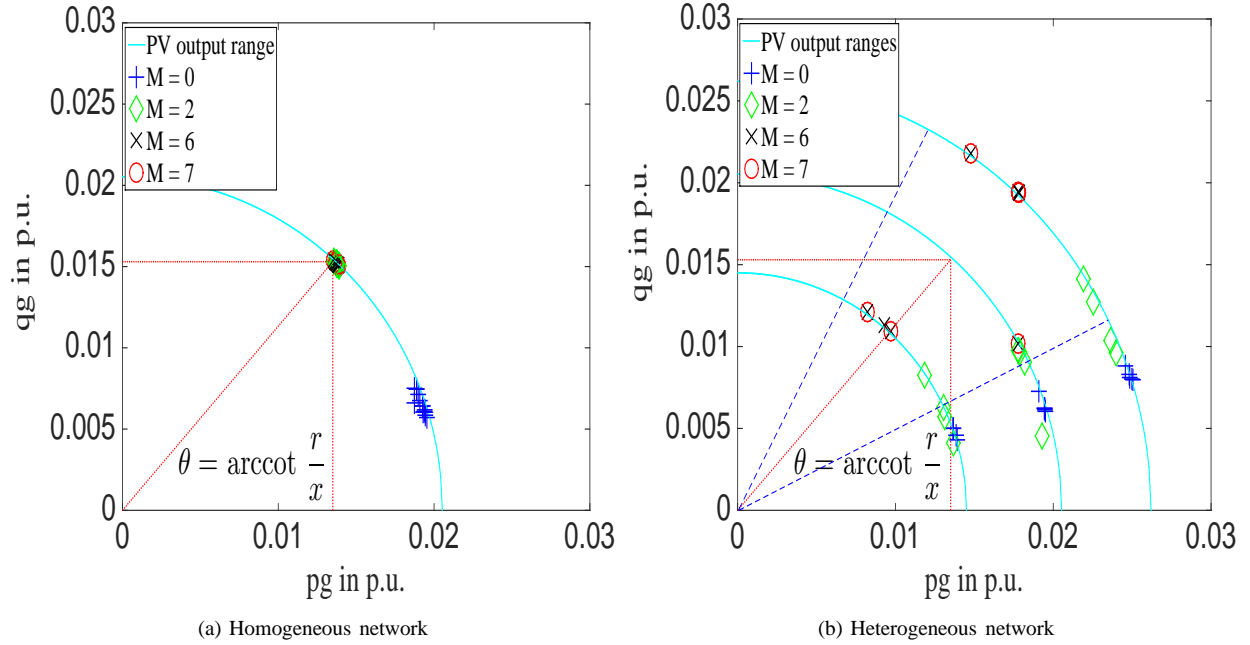


Fig. 8: Reactive Power Vs Real Power Output of DERs.

In our study, we chose $C_i = 7 \text{ cents/kWh}$, converted appropriately to the per unit system.⁷ The ratio $\mathbf{W}/\mathbf{C} = 2$ roughly corresponds to the maximum $\frac{\mathbf{W}}{\mathbf{C}}$ ratio for which the defender does not exercise load control, because the cost of doing load control is too high, i.e., at optimum defender response, $\gamma^* = \mathbf{1}_N$. In contrast, $\mathbf{W}/\mathbf{C} = 18$ roughly corresponds to the minimum $\frac{\mathbf{W}}{\mathbf{C}}$ ratio for which the defender exercises maximum load control (i.e. $\gamma^* = \underline{\gamma}$). We also consider an intermediate ratio, $\mathbf{W}/\mathbf{C} = 10$.

L vs. M. Both L_{VR} and L_{LC} are zero when there is no attack. As M increases, one or both L_{VR} and L_{LC} start increasing. This indicates that as more DERs are compromised, the defender incurs L_{VR} , and in addition, he imposes load control to better regulate the DN. Indeed, after the false set-points (Theorem 2) are used to compromise DERs, the net load in the DN increases. Without load control, the voltages at some nodes drop below the lower bounds, increasing L_{VR} . Hence, the defender exercises load control, and changes the set-points of uncompromised DERs such that $L_{VR} + L_{LC}$ is minimized.

Perhaps the more interesting observation is that as M increases, L_{LC} first increases rapidly but then flattens out. This can be explained as follows. Depending on the $\frac{\mathbf{W}}{\mathbf{C}}$ ratio, there is a subset of downstream loads that are beneficial in terms of the value that defender can obtain by controlling them. That is, if the loads belonging to this subset are controlled, the decrease in L_{VR} outweighs the increase in L_{LC} , hence, the defender imposes load control on these downstream loads to reduce the $L_{VR} + L_{LC}$. In contrast, controlling the loads outside this subset, increases L_{LC} more than the decrease in L_{VR} . Hence, the defender satisfies the demand at these loads fully. Hence, L_{LC} increases until load control capability in the subset of beneficial downstream loads to the defender is fully exhausted. The size of this subset depends on the $\frac{\mathbf{W}}{\mathbf{C}}$ ratio. The higher the ratio, the larger the size of the subset of the loads beneficial to the defender. Hence, the value of M , at which the L_{LC} cost curve flattens out, increases as the $\frac{\mathbf{W}}{\mathbf{C}}$ ratio increases.

The cost curve for L_{VR} also shows interesting behavior as the number of compromised DER nodes increases (Figure 9a and 9b). The marginal increase in L_{VR} for every additional DER compromised reduces as M increases. This observation can be explained by the fact that the attacker prefers to compromise downstream nodes over upstream ones (Proposition 4). Initially, the attacker is able to rapidly increase L by compromising more beneficial downstream nodes. However, as the downstream nodes are eventually exhausted, the attacker has to target the relatively less beneficial upstream nodes. Hence, the reduction in marginal increase of L_{VR} .

In L_{VR} plots, for small M , $\mathbf{W}/\mathbf{C} = 2$ curves are lower than the $\mathbf{W}/\mathbf{C} = 10$ curves which in turn are lower than the $\mathbf{W}/\mathbf{C} = 18$ curves. But, for larger M , this order reverses. The M where these lines cross each other decreases, as the $\underline{\gamma}$

⁷From a practical viewpoint, the weights C_i can be obtained from the operator's rate compensation scheme for load control. For example, North Star Electric [27] provides a compensation of 9.1 cents to their customers for 1 kWh of load curtailment. One can argue that the net cost of shedding unit load should be adjusted to reflect the fact that the defender supplies additional power during the attack to meet the consumers' demand.

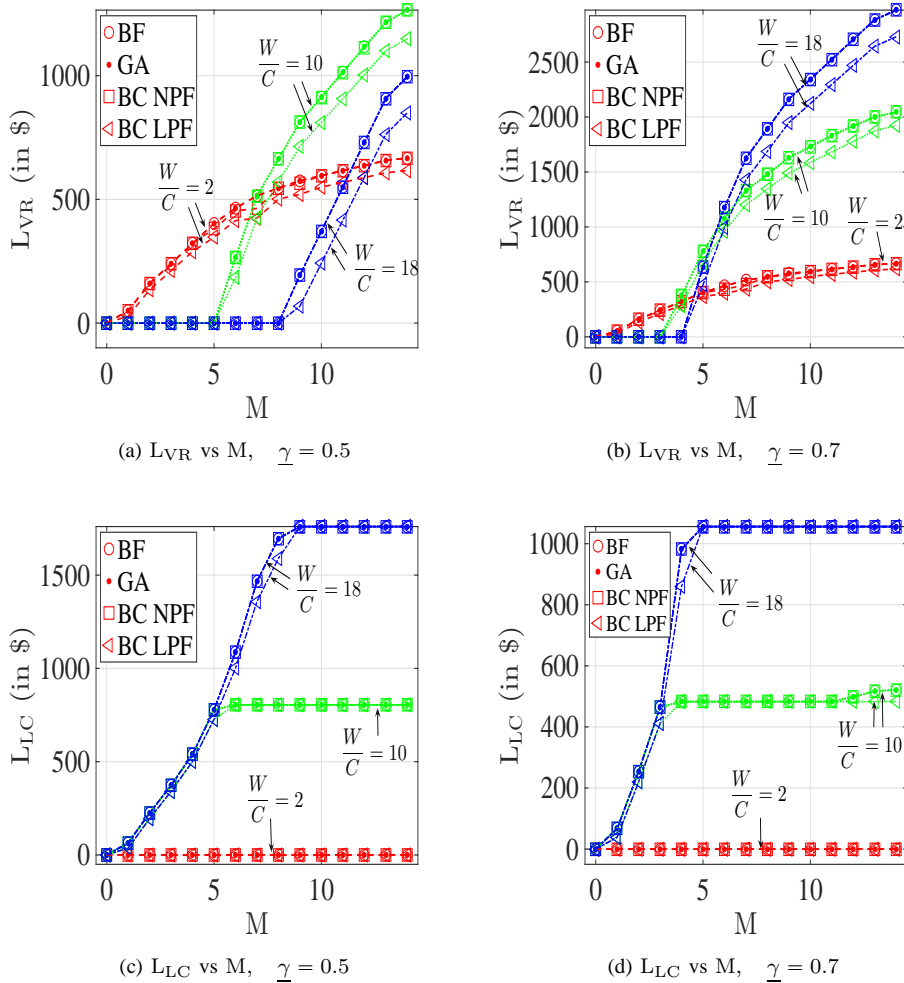


Fig. 9: L_{VR} and L_{LC} vs M for \mathcal{G}^I . The results of \mathcal{G}^H are more or less similar to those of \mathcal{G}^I .

increases. The reason is for some intermediate value of M , the defender exhausts the load control completely, and then the L increases at rates in the same order of increasing W/C values. Finally, for $\underline{\gamma} = 0.7$, the M where defender exhausts the load control completely is smaller than that in $\underline{\gamma} = 0.5$.

The Greedy Approach (GA) is better than Benders Cut (BC) method because GA calculates the exact impact the DER compromises will have on a pivot node. BC overestimates the impact of DER compromises that are not the ancestors to the pivot nodes. Therefore, the feasible region probed by BC at every iteration is larger than the feasible region probed in the corresponding iteration of GA. Hence, although GA converges to a solution in 2-3 iterations, BC in most cases does not converge to the optimal solution even in 200 iterations.

VI. CONCLUDING REMARKS

We focused on the security assessment of tree-like DNs for an adversary model in which multiple DERs (in this case, DER nodes) are compromised. The adversary can be a threat agent, who can compromise the operation of DERs, or a malicious insider in the control center. We considered a composite loss function that primarily accounts for the attacker's impact on voltage regulation and induced load control. The security assessment problem is formulated as a three-stage Defender-Attacker-Defender ([DAD]) sequential game. Our main technical contributions include: (i) Approximating the [DAD] game that has nonlinear power flow model and mixed-integer decision variables with tractable formulations based on linear power flow; and (ii) characterization of structural properties of security investments in Stage 1 and the optimal attack in Stage 2 (i.e., the choice of DER node locations and the choice of false set-points).

Future work includes: (a) Extending Theorems 1 and 2 to cases where reverse power flows are permissible (e.g., when the DN is not under heavy loading conditions and the attacker can cause DER generation to exceed the demand); (b) Designing

greedy algorithm to solve [AD] and proving optimality guarantees of Theorems 3 and 4 for DN with heterogeneous r/x ratio, and heterogeneous DERs or loads. Finally, we believe that the ideas proposed in this paper are also applicable to security assessment of water DN under threats that can cause multiple sources to be compromised and lead to sudden loss in hydraulic head and/or loss of supply to consumers.

We do not consider cascading failures in our paper. However, our analysis can be extended to a form of cascading failures within DN reported by Kundu and Hiskens [28]. They study synchronous tripping of the loads (specifically, plug-in electric vehicles chargers) leading to over-voltages in the DN. Our result on optimal DER attack can be used to create voltage violations at some nodes. If these violations are too high, certain loads may start to trip. After sufficiently large number of loads trip, the attacker can further manipulate the DER setpoints to their maximum power generation capacity. In the absence of new loads, this may lead to overvoltages as described in [28].

REFERENCES

- [1] R. Ma, H.-H. Chen, Y.-R. Huang, and W. Meng, "Smart grid communication: Its challenges and opportunities." *IEEE Trans. Smart Grid*, vol. 4, no. 1, pp. 36–46, 2013. [Online]. Available: <http://dblp.uni-trier.de/db/journals/tsg/tsg4.html#MaCHM13>
- [2] I. A. Hiskens, "What's smart about the smart grid?" in *DAC*, S. S. Sapatnekar, Ed. ACM, 2010, pp. 937–939. [Online]. Available: <http://dblp.uni-trier.de/db/conf/dac/dac2010.html#Hiskens10>
- [3] H. Fawzi, P. Tabuada, and S. Diggavi, "Secure estimation and control for cyber-physical systems under adversarial attacks," *Automatic Control, IEEE Transactions on*, vol. 59, no. 6, pp. 1454–1467, 2014.
- [4] Y. Mo, T. H. jin Kim, K. Brancik, D. Dickinson, H. Lee, A. Perrig, and B. Sinopoli, "Cyber-physical security of a smart grid infrastructure," in *Proceedings of the IEEE*, 2012, pp. 195–209.
- [5] F. Pasqualetti, F. Dörfler, and F. Bullo, "Attack detection and identification in cyber-physical systems," *IEEE Trans. Automat. Contr.*, vol. 58, no. 11, pp. 2715–2729, 2013. [Online]. Available: <http://dx.doi.org/10.1109/TAC.2013.2266831>
- [6] K. C. Sou, H. Sandberg, and K. Johansson, "Computing critical k -tuples in power networks," *Power Systems, IEEE Transactions on*, vol. 27, no. 3, pp. 1511–1520, Aug 2012.
- [7] A. Teixeira, K. C. Sou, H. Sandberg, and K. Johansson, "Secure control systems: A quantitative risk management approach," *Control Systems, IEEE*, vol. 35, no. 1, pp. 24–45, Feb 2015.
- [8] B. A. Robbins and A. D. Domnguez-Garca, "Optimal reactive power dispatch for voltage regulation in unbalanced distribution systems," *IEEE Transactions on Power Systems*, vol. 31, no. 4, pp. 2903–2913, July 2016.
- [9] K. S. Turitsyn, P. Sulc, S. Backhaus, and M. Chertkov, "Options for control of reactive power by distributed photovoltaic generators." *Proceedings of the IEEE*, vol. 99, no. 6, pp. 1063–1073, 2011. [Online]. Available: <http://dblp.uni-trier.de/db/journals/piecee/piecee99.html#TuritsynSBC11>
- [10] J. Salmeron, K. Wood, and R. Baldick, "Analysis of electric grid security under terrorist threat," *Power Systems, IEEE Transactions on*, vol. 19, no. 2, pp. 905–912, May 2004. [Online]. Available: <http://dx.doi.org/10.1109/tpwrs.2004.825888>
- [11] —, "Worst-Case Interdiction Analysis of Large-Scale Electric Power Grids," *Power Systems, IEEE Transactions on*, vol. 24, no. 1, pp. 96–104, Feb. 2009. [Online]. Available: <http://dx.doi.org/10.1109/tpwrs.2008.2004825>
- [12] Y. Yao, T. Edmunds, D. Papageorgiou, and R. Alvarez, "Trilevel optimization in power network defense," *IEEE Transactions on Systems, Man, and Cybernetics, Part C (Applications and Reviews)*, vol. 37, no. 4, pp. 712–718, July 2007.
- [13] A. A. Cárdenas, S. Amin, Z.-S. Lin, Y.-L. Huang, C.-Y. Huang, and S. Sastry, "Attacks against process control systems: Risk assessment, detection, and response," in *Proceedings of the 6th ACM Symposium on Information, Computer and Communications Security*, ser. ASIACCS '11. New York, NY, USA: ACM, 2011, pp. 355–366. [Online]. Available: <http://doi.acm.org/10.1145/1966913.1966959>
- [14] M. Farivar, R. Neal, C. R. Clarke, and S. H. Low, "Optimal inverter var control in distribution systems with high pv penetration," *CoRR*, vol. abs/1112.5594, 2011. [Online]. Available: <http://dblp.uni-trier.de/db/journals/corr/corr1112.html#abs-1112-5594>
- [15] A. Lee, "Electric sector failure scenarios and impact analyses," National Electric Sector Cybersecurity Organization Resource (NESCOR), Electric Power Research Institute (EPRI), Palo Alto, California, Tech. Rep., June 2014. [Online]. Available: <http://www.smartgrid.epri.com/doc/NESCOR/%20failure%20scenarios%2006-30-14a.pdf>
- [16] R. Lee, M. Assante, and T. Conway, "Analysis of the cyber attack on the ukrainian power grid, electricity information sharing and analysis center," http://www.nerc.com/pa/CI/ESISAC/Documents/E-ISAC_SANS_Ukraine_DUC_18Mar2016.pdf, 2015.
- [17] R. Campbell, "Cybersecurity issues for the bulk power system, congressional research service report," <https://www.fas.org/sgp/crs/misc/R43989.pdf>, 2015.
- [18] H.-D. Chiang and M. Baran, "On the existence and uniqueness of load flow solution for radial distribution power networks," *Circuits and Systems, IEEE Transactions on*, vol. 37, no. 3, pp. 410–416, Mar 1990.
- [19] E. Dall'Anese and G. B. Giannakis, "Sparsity-leveraging Reconfiguration of Smart Distribution Systems," *ArXiv e-prints*, Mar. 2013.
- [20] D. Shelar and S. Amin, "Analyzing vulnerability of electricity distribution networks to DER disruptions," in *American Control Conference, ACC 2015, Chicago, IL, USA, July 1-3, 2015*, 2015, pp. 2461–2468. [Online]. Available: <http://dx.doi.org/10.1109/ACC.2015.7171101>
- [21] M. Farivar and S. H. Low, "Branch flow model: Relaxations and convexification." in *CDC. IEEE*, 2012, pp. 3672–3679. [Online]. Available: <http://dblp.uni-trier.de/db/conf/cdc/cdc2012.html#FarivarL12>
- [22] S. Amin, G. A. Schwartz, and S. Shankar Sastry, "Security of interdependent and identical networked control systems," *Automatica*, vol. 49, no. 1, pp. 186–192, Jan. 2013. [Online]. Available: <http://dx.doi.org/10.1016/j.automatica.2012.09.007>
- [23] D. Shelar, J. Giraldo, and S. Amin, "A distributed strategy for electricity distribution network control in the face of DER compromises," in *CDC. IEEE*, 2015, pp. 6934–6941.
- [24] D. Shelar and S. Amin, "Security assessment of electricity distribution networks under der node compromises," 2015. [Online]. Available: <https://arxiv.org/abs/1601.01342v2>
- [25] R. Wood, "Bilevel network interdiction models: Formulations and solutions," in *Wiley Encyclopedia of Operations Research and Management Science*, 2011.
- [26] L. Gan, N. Li, U. Topcu, and S. Low, "Exact convex relaxation of optimal power flow in radial networks," *Automatic Control, IEEE Transactions on*, vol. 60, no. 1, pp. 72–87, Jan 2015.

| Parameters | Values |
|----------------------------|----------------------------------|
| $r + \mathbf{j}x$ | $(0.33 + 0.38\mathbf{j}) \Omega$ |
| pc_i^{nom} | 15 kW |
| qc_i^{nom} | 4.5 kvar |
| $\widehat{\text{sp}}_i$ | 11.55 kVA |
| $ V_0 $ | 4 kV |
| C | $7 \text{ \$ per kW}$ |

TABLE II: Parameters of the Homogeneous Network

[27] "Compensation of load control." [Online]. Available: http://www.northstarelectric.coop/?page_id=180

[28] S. Kundu and I. Hiskens, "Overvoltages due to synchronous tripping of plug-in electric-vehicle chargers following voltage dips," *Power Delivery, IEEE Transactions on*, vol. 29, no. 3, pp. 1147–1156, June 2014.

APPENDIX

For a pivot node $i \in \mathcal{N}$, Algorithm 5 computes a sequence of sets of nodes in decreasing order of $\Delta_j(\widehat{v}_i)$ values. This sequence is used to compute the optimal attacks that maximize voltage bounds violation at node i .

Algorithm 5 Helper procedures

-
- 1: **procedure** OPTIMALATTACKHELPER($i, \widehat{\text{sp}}^{\text{d}}$)
 - 2: For each $j \in \mathcal{N}$ compute $\Delta_j(\widehat{v}_i)$ using Lemma 4
 - 3: Create a sequence of sets $\{\mathcal{N}_j^i\}_{j=1}^N$ such that
 - i) $\mathcal{N} = \bigcup_{j=1}^N \mathcal{N}_j^i, \forall 1 \leq j, k \leq N, \mathcal{N}_j^i \cap \mathcal{N}_k^i = \emptyset$
 - ii) if $1 \leq l \leq N, j, k \in \mathcal{N}_l^i$, then $\Delta_j(\widehat{v}_i) = \Delta_k(\widehat{v}_i)$, and
 - iii) if $1 \leq l < m \leq N, j \in \mathcal{N}_l^i, k \in \mathcal{N}_m^i$, then $\Delta_j(\widehat{v}_i) > \Delta_k(\widehat{v}_i)$.
 - 4: Let, for $j \in [1, \dots, N], m_j^i \leftarrow |\mathcal{N}_j^i|, M_j^i := \sum_{k=1}^{j-1} m_k^i$.
 - 5: Let $g^i \leftarrow \operatorname{argmin}_{j \in [1, \dots, N], M_j^i \geq M} j$.
 - 6: $J \leftarrow \bigcup_{j=1}^{g^i-1} \mathcal{N}_{g^i}^i, m' = M - M_{g^i-1}^i$
 - 7: **return** $J, \mathcal{N}_{g^i}^i, m'$
 - 8: **end procedure**
-

Proof of Lemma 3. Let $[\widetilde{\text{AD}}]^{\text{d}}$ denote the following problem:

$$[\widetilde{\text{AD}}]^{\text{d}} \quad \tilde{\phi}^*(\psi) \in \operatorname{argmin}_{\phi \in \Phi} L(x(\psi, \phi)) \quad \text{s.t.} \quad \widehat{x}(u, \psi, \phi) \in \mathcal{X}_{\text{CPF}}, (8\text{b}), (8\text{c}). \quad (40)$$

(A0)₁ implies that a feasible solution exists for $[\text{AD}]^{\text{d}}$. Since, $\mathcal{X} \subset \mathcal{X}_{\text{CPF}}$, a feasible solution $\tilde{x} \in \mathcal{X}_{\text{CPF}}$ also exists for $[\widetilde{\text{AD}}]^{\text{d}}$.

Let $(\tilde{\phi}, \tilde{\ell})$ denote the decision variables for $[\widetilde{\text{AD}}]^{\text{d}}$. Note that, for a fixed ψ , \tilde{x} is affine in the variables $(\tilde{\phi}, \tilde{\ell})$, and can be very efficiently computed using (5a) and (5b).

Now, L is convex in $\tilde{\phi}$ (because the L_{VR} is a maximum over affine functions, L_{LC} is affine in $\tilde{\phi}$, and L_{LL} is affine in $\tilde{\ell}$). Also, Φ is a convex compact set. Further, for a fixed ϕ , L is strictly increasing in $\tilde{\ell}$ (because, L_{VR} is non-decreasing in $\tilde{\ell}$ as \tilde{v} is affine decreasing in $\tilde{\ell}$; L_{LC} does not change with $\tilde{\ell}$; L_{LL} is strictly increasing in ℓ). From Thm. 1 [21], $(\tilde{\phi}^*, \tilde{\ell}^*)$ can be computed using a SOCP. To argue that $\tilde{\ell}^*$ satisfy (5c), assume for contradiction that $\exists (i, j) \in \mathcal{E}$, s.t. $\tilde{\ell}_j^* > |\tilde{s}_j^*|^2/\tilde{v}_i^*$. Then, construct $(\phi^*, \tilde{\ell}')$ such that $\forall j \in \mathcal{N} : j \neq i, \tilde{\ell}'_j = \tilde{\ell}_j^*$, and $\tilde{\ell}'_i = |\tilde{s}_j^*|^2/\tilde{v}_i^*$. Since $\forall (j, k) \in \mathcal{E}, |\tilde{s}_k|^2/\tilde{v}_j$ is strictly decreasing in $\tilde{\ell}_i, \forall (j, k) \in \mathcal{E} : \tilde{\ell}'_k \geq |\tilde{s}_k^*|^2/\tilde{v}_j^* > |\tilde{s}_k^*|^2/\tilde{v}_j'$. Hence, one can further minimize the loss function by choosing a new feasible solution $(\phi^*, \tilde{\ell}')$, thus violating the optimality of $(\tilde{\phi}^*, \tilde{\ell}^*)$. ■

Proof of Proposition 2. Let (d_i, θ_i) denote $\widehat{\text{sp}}_i^{\text{d}}$ in the polar coordinates, i.e., $d_i = |\widehat{\text{sp}}_i^{\text{d}}|, \theta_i = \angle \widehat{\text{sp}}_i^{\text{d}}$.

For $\delta_i = 0, \widehat{\text{sp}}_i = \widehat{\text{sp}}_i^{\text{d}}$. Then from (19a), $\forall j \in \mathcal{N}$,

$$\widehat{v}_j = \widehat{v}'_j + 2d_i(R_{ij} \cos \theta_i + X_{ij} \sin \theta_i), \quad (41)$$

where $\widehat{v}'_j = \nu_0 - 2 \sum_{k \in \mathcal{N}, k \neq j} \operatorname{Re}(\bar{Z}_{jk} s_k) - 2 \operatorname{Re}(\bar{Z}_{ij} s_j)$. Note that \widehat{v}'_j does not depend on (d_i, θ_i) .

It is clear from (41) that $\hat{\nu}_j$ is greater if $\theta_i \in [0, \pi/2]$ than if $\theta_i \in [-\pi/2, 0]$. Furthermore, the impedances are positive. Hence, $\forall j, \partial_{d_i} \hat{\nu}_j = 2(R_{ij} \cos \theta_i + X_{ij} \sin \theta_i) > 0$. Hence, $\partial_{d_i} L_{VR} > 0$. But, from (4), $d_i \leq \overline{\text{sp}}_i$. Hence, $d_i^* = \overline{\text{sp}}_i$. Further, $\partial_{\theta_i} \hat{\nu}_j = 2d_i(-R_{ij} \sin \theta_i + X_{ij} \cos \theta_i)$.

$$\partial_{\theta_i} \hat{\nu}_j \begin{cases} > 0 & \text{if } \theta_i \in [0, \arccot(R_{ij}/X_{ij})] \\ = 0 & \text{if } \theta_i = \arccot(R_{ij}/X_{ij}) \\ < 0 & \text{if } \theta_i \in (\arccot(R_{ij}/X_{ij}), \pi/2] \end{cases}$$

Now, $\arccot \overline{K} \leq \arccot(X_{ij}/R_{ij}) \leq \arccot \underline{K}$. Hence,

$$\forall j \in \mathcal{N}, \quad \partial_{\theta_i} \hat{\nu}_j \begin{cases} < 0 & \text{if } \theta_i > \arccot \underline{K} \\ > 0 & \text{if } \theta_i < \arccot \overline{K} \end{cases} \quad (42)$$

Suppose, for contradiction, $\theta_i^* \notin [\arccot \overline{K}, \arccot \underline{K}]$. Holding all else equal, for $\theta_i = \tilde{\theta}_i$, let $\hat{\nu}(\tilde{\theta}_i)$ and $L_{VR}(\tilde{\theta}_i)$ be the $\hat{\nu}$ and L_{VR} . From (42), for any $\tilde{\theta}_i \in [\arccot \overline{K}, \arccot \underline{K}]$, $\hat{\nu}(\tilde{\theta}_i) > \hat{\nu}(\tilde{\theta}_i^*)$. Since, $L_{VR} > L_{LL} \geq 0$, $L_{VR}(\tilde{\theta}_i) < L_{VR}(\tilde{\theta}_i^*)$, violating the optimality of $\tilde{\theta}_i^*$. Furthermore, under identical \mathbf{r}/\mathbf{x} ratio, $\underline{K} = \overline{K} = K$, which implies $\theta_i = \arccot K$. ■

Proof of Lemma 4. Let sp_j be the DER set-point of node j before the attack. If sp_j is the pre-attack set-point, let $\Delta_j(\text{sp}_j)$ denote the change in the set-point of DER j after it is compromised. By Theorem 2, $\Delta(\text{sp}_j) = \text{sp}_j - \text{sp}_j^a = \text{sp}_j - (0 - \mathbf{j}\overline{\text{sp}}_j) = \text{sp}_j + \mathbf{j}\overline{\text{sp}}_j$; and by linearity in (19a),

$$\Delta_j(\nu_i) = 2\text{Re}(\bar{Z}_{ij}\Delta_j(\text{sp}_j)) = 2\text{Re}(\bar{Z}_{ij}(\text{sp}_j^d + \mathbf{j}\overline{\text{sp}}_j)).$$

Again, by invoking the linearity in (19a), (27a) follows.

Similarly, one can show (26b) and (27b). ■

Proof of Proposition 4. When $\delta_j = 1$, i.e., the DER j is compromised, only the power supplied at node j changes. Using (26a), we get,

$$\begin{aligned} \therefore \Delta_j(\hat{\nu}_i) &= 2\text{Re}(\bar{Z}_{ij}\Delta(\text{sp}_j^d)) \\ &= 2\text{Re}(\bar{Z}_{ij}(\text{sp}_j^d + \mathbf{j}\overline{\text{sp}}_j)) \end{aligned}$$

$$\text{Now, } j <_i k \implies \mathcal{P}_i \cap \mathcal{P}_j \subset \mathcal{P}_i \cap \mathcal{P}_k \implies Z_{ij} < Z_{ik}.$$

$$\begin{aligned} \therefore \Delta_j(\hat{\nu}_i) &= 2\text{Re}(\bar{Z}_{ij}(\text{sp}_j^d + \mathbf{j}\overline{\text{sp}}_j)) \\ &< 2\text{Re}(\bar{Z}_{ik}(\text{sp}_k^d + \mathbf{j}\overline{\text{sp}}_k)) = \Delta_k(\hat{\nu}_i) \end{aligned}$$

Similarly, we can prove the case for $j =_i k$.

Under the ϵ -LPF model, $\Delta_j(\tilde{\nu}_i) = 2(1 + \epsilon)\text{Re}(\bar{Z}_{ij}(\text{sp}_j^d + \mathbf{j}\overline{\text{sp}}_j))$. The rest of the proof follows similarly. ■

Refer to Figure 7c for the purpose of proofs of Propositions 7 to 9.

Proof of Proposition 7. Let (δ^*, ϕ^*) and $(\tilde{\delta}^*, \tilde{\phi}^*)$, denote the optimal solutions of $[\widehat{\text{AD}}]$ with $u = \hat{u}$ (resp. $u = \tilde{u}$). (A1) $\implies \text{sp}^{d^*}$ is fixed (Proposition 2). Hence, ϕ^* depends only on δ^* , and not u . Then, let $\phi^*(\delta)$ denote optimal defender response to δ . We want to show $\hat{\mathcal{L}}^{\tilde{u}} \leq \hat{\mathcal{L}}^u$.

Case $\tilde{\delta}_a^* = 0$. Then $\tilde{\delta}^* \in \mathcal{D}_M(u)$. Thus,

$$\begin{aligned} \hat{\mathcal{L}}^{\tilde{u}} &= \hat{L}(\hat{\mathbf{x}}(\tilde{u}, \tilde{\delta}^*, \phi^*(\tilde{\delta}^*))) \\ &= \hat{L}(\hat{\mathbf{x}}(u, \tilde{\delta}^*, \phi^*(\tilde{\delta}^*))) \\ &\leq \hat{L}(\hat{\mathbf{x}}(u, \delta^*, \phi^*(\delta^*))), \end{aligned}$$

where the inequality follows due to the optimality of δ^* .

Case $\tilde{\delta}_a^* = 1$. Let $\delta \in \mathcal{D}_M(u) : \delta_a = 0, \delta_b = 1, \forall i \in \mathcal{N} \setminus \{a, b\}, \delta_i = \tilde{\delta}_i^*$. We have assumed that $b \in \Lambda_a$; see Figure 7c. Therefore, $\forall i \in \mathcal{N}, a \leq_i b$. Hence, by Proposition 4,

$$\forall i \in \mathcal{N}, \quad \Delta_b(\hat{\nu}_i) \geq \Delta_a(\hat{\nu}_i).$$

Then, by Lemma 4, for fixed ϕ , $\Delta_\delta(\hat{\nu}) \geq \Delta_{\tilde{\delta}^*}(\hat{\nu})$. Hence,

$$\begin{aligned} \widehat{\mathcal{L}}^{\tilde{u}} &= \widehat{\mathcal{L}}(\widehat{\mathbf{x}}(\tilde{u}, \tilde{\delta}^*, \phi^*(\tilde{\delta}^*))) \\ &\leq \widehat{\mathcal{L}}(\widehat{\mathbf{x}}(\tilde{u}, \tilde{\delta}^*, \phi^*(\delta))) \\ &\leq \widehat{\mathcal{L}}(\widehat{\mathbf{x}}(u, \delta, \phi^*(\delta))) \\ &\leq \widehat{\mathcal{L}}(\widehat{\mathbf{x}}(u, \delta^*, \phi^*(\delta^*))) \\ &= \widehat{\mathcal{L}}^u \end{aligned}$$

Here, the first (resp. last) inequality follows due to optimality of $\phi^*(\tilde{\delta}^*)$ (resp. δ^*). Hence, $u \leq \tilde{u}$. ■

Proof of Proposition 8. Let $c = \operatorname{argmax}_{(i \in \mathcal{P}_a \cap \mathcal{P}_b)} h_i$, be the lowest common ancestor of a and b . Let $i', i'' \in \mathcal{N}_c^c : a \in \Lambda_{i'}$ and $b \in \Lambda_{i''}$. From Theorem 3, we know that the optimal attack δ^* will be a pivot node attack $\widehat{\delta}^i$ for some node, say $i \in \mathcal{N}$. Let $\mathcal{N}' = \Lambda_{i'} \cup \Lambda_{i''}$.

Case $i \in \mathcal{N}'$. Now $u_j = 1 \forall j \in \Lambda_{i'} \setminus \Lambda_{i'}^a \cup \{a\}$ by maximality of $|\mathcal{P}_a \cap \mathcal{P}_b|$. Similarly, $u_j = 0 \forall j \in \Lambda_{i''}^d \cup \{b\}$. Thus, $\forall j \in \Lambda_{i'}$ s.t. $u_j = 0$ there exists a separate node $k \in \Lambda_{i''}$ such that j and k are homomorphic, and $u_k = 0$ (see Figure 7c). Hence, the subtree $\Lambda_{i''}$ is more vulnerable than the subtree $\Lambda_{i'}$, and it will be more beneficial for the attacker to target a pivot node in $\Lambda_{i''}$. Now, $i \in \Lambda_{i''}$, and $\forall i \in \Lambda_{i''}$, $a <_i b$. Hence, by using Proposition 4, we get, $\Delta_a(\widehat{\nu}_i) < \Delta_b(\widehat{\nu}_i)$.

Case $i \notin \mathcal{N}'$. Then $a =_i b$, and by Proposition 4, $\Delta_a(\widehat{\nu}_i) = \Delta_b(\widehat{\nu}_i)$.

We now want to show that $\widehat{\mathcal{L}}^{\tilde{u}} \leq \widehat{\mathcal{L}}^u$. The rest of the proof follows along the same lines as the proof of Proposition 7. ■

Proof of Proposition 9. Similar to the proof of Proposition 8. ■

| | | | |
|---------------------------------------|--|--|---|
| \mathbf{j} | $\mathbf{j} = \sqrt{-1}$ complex square root of -1 | | |
| Network parameters | | | |
| \mathcal{N} | Set of nodes | | |
| \mathcal{E} | Set of edges | | |
| \mathcal{G} | Tree topology $\mathcal{G} = (\mathcal{N}, \mathcal{E})$ | | |
| r_j | resistance of line $(i, j) \in \mathcal{E}$ | | |
| x_j | reactance of line $(i, j) \in \mathcal{E}$ | | |
| z_j | impedance $z_j = r_j + \mathbf{j}x_j$ of line $(i, j) \in \mathcal{E}$ | | |
| H | height of the tree | | |
| \mathcal{N}_h | set of nodes on level $h \in 1, 2, \dots, H$ | | |
| h_i | level of node i | | |
| \mathcal{N}_i^c | set of children nodes of node i | | |
| Λ_i | subtree rooted at node $i \in \mathcal{N}$ | | |
| Λ_i^j | subtree rooted at node $i \in \mathcal{N}$ until level h_j for $j \in \Lambda_i$ | | |
| \mathcal{P}_i | path from the root node to node i | | |
| Z_{ij} | $Z_{ij} := \sum_{k \in \mathcal{P}_i \cap \mathcal{P}_j} z_k$ common path impedances between nodes i and j | | |
| Power flow notations | | | |
| NPF | Nodal quantities of node $i \in \mathcal{N}$ | | LPF ϵ -LPF |
| sc_i^{nom} | complex power demand at node i | | — — |
| sc_i | complex power consumed at node i | | \hat{sc}_i \check{sc}_i |
| sg_i | complex power generated at node i | | \hat{sg}_i \check{sg}_i |
| sp_i | complex power set-point of DER i | | \hat{sp}_i \check{sp}_i |
| V_i | complex voltage at node i | | \hat{V}_i \check{V}_i |
| ν_i | square of voltage magnitude at node i | | $\hat{\nu}_i$ $\check{\nu}_i$ |
| $\underline{\nu}_i, \overline{\nu}_i$ | <i>soft</i> lower and upper bounds on square of voltage magnitude at node i | | |
| NPF | Edge quantities of edge $(i, j) \in \mathcal{E}$ | | LPF ϵ -LPF |
| S_j | complex power flowing on line (i, j) | | \hat{S}_i \check{S}_i |
| I_j | complex current flowing on line (i, j) | | \hat{I}_i \check{I}_i |
| ℓ_j | square of magnitude of current I_j | | $\hat{\ell}_i$ $\check{\ell}_i$ |
| \mathbf{x} | $\mathbf{x} = (\nu, \ell, sc, sg, S)$ - state vector | | $\hat{\mathbf{x}}$ $\check{\mathbf{x}}$ |
| Attacker model | | | |
| δ_i | $\delta_i = 1$ if DER i is compromised | | — — |
| sp_i^a | attacker set-point of DER i | | \hat{sp}_i^a \check{sp}_i^a |
| ψ | $\psi := (sp^a, \delta)$ attacker strategy | | $\hat{\psi}$ $\check{\psi}$ |
| Defender model | | | |
| $\underline{\gamma}_i$ | max. allowed fraction of load control | | — — |
| γ_i | fraction of load control at load i | | $\hat{\gamma}_i$ $\check{\gamma}_i$ |
| sp_i^d | defender set-point of DER i | | \hat{sp}_i^d \check{sp}_i^d |
| ϕ | $\phi := (sp^d, \gamma)$ defender strategy | | $\hat{\phi}$ $\check{\phi}$ |

TABLE III: Table of Notations